THE ICING PROBLEM: CURRENT STATUS OF NACA TECHNIQUES

AND RESEARCH

Uwe H. von Glahn
National Advisory Committee for Aeronautics
Cleveland, Ohio

THE ICING PROBLEM - CURRENT STATUS OF NACA TECHNIQUES AND RESEARCH

By Uwe H. von Glahn

National Advisory Committee for Aeronautics
Lewis Flight Propulsion Laboratory
Cleveland, Ohio

Icing of aircraft components such as airfoil surfaces and engine-inlet systems similar to those shown in figure 1 creates a serious operational problem. Aircraft are now capable of flying in icing clouds without difficulty, however, because research by the NACA and others has provided the engineering basis for icing protection systems. This paper summarizes some of the techniques used in NACA programs to solve aircraft icing problems and indicates the scope of the data available for the design of aircraft icing protection systems. In addition, appendixes A to C discuss the NACA Lewis icing facilities in detail, specific test equipment and techniques used in conducting tests in icing wind tunnels, and several icing instruments.

Icing of aircraft surfaces occurs when liquid cloud droplets cooled below the freezing temperature impinge on a surface that is also below freezing. All surfaces that are exposed to the direct impingement of supercooled water droplets therefore may require icing protection (fig. 2). The size and extent of icing on an airplane component is a function of cloud liquid-water content, droplet size, and air temperature, physical dimensions and shape of the component (size, shape, and attitude), and operating conditions (airspeed and altitude).

A body moving through a cloud of water droplets, in general, will not intercept all the droplets originally contained in the volume of air swept out by the projected frontal area of the body (fig. 3). As the droplets reach the vicinity of the body, the air streamlines flow around the body. The droplets, because of their momentum, tend to maintain straight paths toward the body; however, a drag force imposed by the relative velocity of the air with respect to a droplet tends to cause the droplet to follow the air streamlines. The relative magnitudes of the momentum and drag forces determine the droplet path. The path of droplets in the flow field can be determined analytically with particle trajectory equations. In order to do this, however, the size of the cloud droplets must be known. This information has been obtained with instrumented aircraft in flight through icing clouds. Two of the most widely used methods of obtaining cloud icing data are rotating multicylinders and the pressure-type icing-rate meter.

The rotating-multicylinder method has been used extensively to collect data on both droplet-size distribution and liquid-water content in supercooled clouds (refs. 1 to 4). The collection of ice by the cylinders is similar to the collection of ice by airplane components. Therefore, the

data obtained by this method have been valuable in designing icing pro-
tection systems for airplanes. In this method, several cylinders of dif-
ferent diameter rotating on a common axis are exposed from an aircraft in
flight or in an icing tunnel to supercooled cloud droplets as shown in
figure 4. During the exposure period, the cylinders collect ice. The
cylinders are rotated in order to obtain uniform ice collection around
the circumference and thereby to preserve a circular cross section.

After exposure, the diameters of the iced cylinders are measured and
the iced cylinders are weighed. The measurement of droplet size and water
content is based on the principle that cylinders of different sizes collect
different quantities of ice per unit frontal area. The ice collection of
each cylinder is expressed in terms of a collection efficiency that has
been obtained theoretically. The liquid-water content, average droplet
size, and droplet-size distribution are obtained by a comparison of the
measured weight of ice collected on each cylinder with calculated values
of collection efficiency. The method is applicable only in cloud where
the temperature is below 0° C.

The pressure-type instrument (ref. 5) operates on the differential
pressure created when small total-pressure holes plug with ice accretions,
as illustrated in the sketch of figure 5. The small total-pressure holes
in the ice-collecting element, which are vented to static pressure through
a small orifice, are balanced against a non-vented, ice-free total pressure
in a differential pressure switch. When these small total-pressure holes
plug from ice accretion, the pressure in the corresponding side of the
pressure switch approaches static by bleeding through the static orifice,
and a differential pressure is created between the iced and ice-free
systems. Continuous operation is obtained by allowing the differential
pressure switch to energize an electrical heater that de-ices the ice-
plugged total-pressure holes. The pressures in the two systems then tend
to equalize, opening the pressure switch and allowing the cycle to be re-
peated. The heat-off time of this cyclic process is used as a measure of
the period of time required to plug the holes. This period of time is a
function of the rate at which ice accumulates on the element containing
the holes, because the amount of ice accretion required for plugging is a
constant value. The duration of the heat-off period is calibrated against
a measured icing rate. An NACA flight-type film recorder is used to re-
cord continuously the duration of the heat-off or icing period, the heat-
on or de-icing period, the indicated airspeed, the air temperature, and
the altitude. The icing rate is then used to calculate the water content
of the icing cloud. This instrument is limited by water run-off at air
temperatures near 0° C and high water contents, as are the rotating multi-
cylinders. Also, it does not measure droplet size. Other icing instru-
ments are discussed in appendix C.

In general, the average droplet size in icing clouds is in the range
of 10 to 25 microns in diameter. In stratus clouds the maximum water
content is about 1.5 grams per cubic meter, while in cumulus clouds the

water content may be as high as 3.5 grams per cubic meter. Fortunately, these high water contents extend over only a short horizontal distance. For cumulus clouds the extent of such high water contents is only about 1/2 mile, while for stratus clouds the high water contents usually do not exceed 10 to 20 miles.

The data obtained by the rotating-multicylinder method have been of significance in establishing meteorological design criteria for aircraft icing protection systems. These data, however, were based on flights by only a few aircraft in deliberately sought icing conditions. The data from the pressure-type meter have been obtained on a routine flight basis by a cooperative program between the NACA, commercial airlines, and the United States Air Force. Some 50 aircraft were instrumented with these meters in various geographical areas of the world (fig. 6), including the North Atlantic, the continental United States, Alaska, the Pacific, and Japan. In addition, the program has been supplemented by in-flight weather reconnaissance reports form the Air Weather Service and Strategic Air Command aircraft over a two-year period. These data have been put on punch cards and are currently being analyzed on IBM equipment. Because most of the data obtained from routine flights apply to low altitudes, special efforts are being made to obtain data on the occurrence of icing at altitudes above 20,000 feet. Data obtained to date show that icing is rarely encountered about 30,000 feet because of the infrequency of clouds containing liquid water at the low temperatures associated with these altitudes. In addition, the severity of icing encountered above 30,000 feet is usually low except in scattered thunderstorm clouds.

The impingement characteristics and the initial rate of ice forma- tion on aircraft components can be obtained by either theoretical tra- jectory studies or experimental means, once the water content and droplet sizes of icing clouds are available. Most of the NACA analytical studies of droplet trajectories about various bodies (refs. 6 to 13) utilize a differential analyzer (fig. 7), since experience has shown that even the simplest manual calculations are time-consuming and inaccurate. The use of the differential analyzer in this work is described in reference 14.

Typical results obtained from such a trajectory study are shown in figure 8, in which the local impingement rate on an airfoil is plotted as a function of surface distance from the leading edge. The data shown are for a 15-percent symmetrical airfoil of 8-foot chord, angle of attack of zero, airspeed of 150 knots, and average droplet sizes of 8 and 15 microns. The greatest impingement occurs at the stagnation region and decreases rapidly with surface distance from the leading edge. An increase in aver- age droplet size from 8 to 15 microns increases the local impingement rates and causes the impingement area to extend farther aft than with the smaller droplets.

The differential analyzer is difficult to use for droplet trajectories about bodies with complex air flows. Therefore, a wind-tunnel method using

a dye-tracer technique (ref. 15) is often used to obtain experimentally
the droplet impingement on these bodies. In this technique (fig. 9),
water treated with known small quantities of water-soluble dye is sprayed
into the airstream a large distance ahead of the body by nozzles. The
surface of the body is covered with blotter paper upon which the dyed
water droplets impinge and are absorbed. At the point of droplet impact,
a permanent dye trace is obtained. The amount of dye obtained in a meas-
ured time interval can be determined by a colorimetric analysis of
punched-out segments of blotted paper (fig. 9) and converted into the
quantity of water that produced the dye trace. The maximum extent of im-
pingement of the local dye or water deposit over the entire wetted sur-
face will yield the total amount of water collected by the body. This
experimental technique requires a knowledge of the droplet-size distribu-
tion and water content of the spray cloud. Methods of obtaining these
parameters have been worked out and are included in the report concerning
the technique (ref. 15).

The total water catch and the extent of impingement on an airfoil
surface obtained by the differential analyzer are compared in figure 10
with the experimental data (unpublished). These data are shown as a func-
tion of an impingement parameter which, in this case, depends primarily
on the droplet size squared, wing chord, and airspeed (ref. 16). These
are typical results for a 15-percent-thick symmetrical wing at zero angle
of attack.

From a knowledge of the droplet impingement characteristics and
meteorological parameters, the local water impingement rate or icing
rate on component surfaces can be calculated. Unfortunately, the shape
of the resultant ice formation, which has a large effect on the aerody-
namic penalties associated with component icing, can only be estimated
based on limited experimental data, since the ice-formation shape is
also a function of airfoil sweep angle, air temperature, and aircraft
speed. Ice shapes can be generalized into two primary shapes, rime icing
and heavy glaze icing (fig. 11). Rime icing is associated primarily with
low air temperatures and results in relatively streamlined ice formations
that blend into the body shape and cause little aerodynamic penalty.
Heavy glaze icing results from high water contents, large droplets, and
surface temperatures near freezing. This combination of meteorological
conditions causes rough ice formations that protrude from the body sur-
faces into the airstream and cause large aerodynamic penalties.

Early attempts to measure these penalties were made in flight through
icing clouds. However, the general advantages of doing icing research in
a tunnel where conditions can be controlled were recognized, and an icing
research tunnel was built at the NACA Lewis laboratory. The Lewis icing
tunnel is a single-return closed-throat tunnel, the general arrangement of
which is shown in figure 12. The test section is rectangular in shape,
9 feet wide, 6 feet high, and 20 feet long. The maximum tunnel airspeed

with icing conditions and with a large model in the test section is about 260 knots. Air temperatures as low as -40° C can be obtained, although most tests are conducted in the range of -3° to -20° C.

Icing conditions similar to those encountered in the atmosphere are created by a battery of air-water atomizing nozzles. A view of the spray system looking downstream into the test section is shown in figure 13. The spray nozzles are mounted in six horizontal spray bars and located to give a uniform cloud approximately 4- by 4-feet in the test section. This cloud conforms to natural icing clouds measured in flight. Details of this icing tunnel, its equipment and instrumentation, as well as of several high-speed icing duct tunnels, are given in appendixes A and B.

In order to determine the magnitude of the aerodynamic penalties associated with icing of lifting surfaces, airfoils of different sizes, thicknesses, and shapes were tested in the Lewis icing tunnel over a wide range of angles of attack and icing conditions (refs. 17 and 18). Section-drag measurements during icing were obtained by means of an integrating wake survey rake (fig. 14) and the tunnel force-measuring balance system. Lift and pitching moments were also measured with the balance system.

A typical lift and drag curve for an NACA 0011 airfoil at an angle of attack of 2.3° is shown in figure 15 as a function of time in glaze icing, together with a picture of the ice formation at the end of 18 minutes of icing (unpublished data). It is apparent that under these operating conditions the loss in lift of 12 percent and the increase in section drag of 270 percent after 18 minutes of icing could constitute a serious problem for an aircraft.

Ice formations on aircraft components can be prevented by flowing or spraying temperature-depressant fluids over the component surfaces (ref. 19) or by heating the surfaces (refs. 18 to 23). The work of the NACA has emphasized the use of heat for icing protection. Component icing can be prevented by thermal means in two ways: (1) The surfaces can be raised to a temperature just sufficient to maintain the impinging water in a liquid state over the entire surface, or (2) the surfaces can be supplied sufficient heat to evaporate the impinging water in a specified distance aft of the impingement area while the remainder of the surface is unheated. Obviously, it takes more heat per unit surface area to evaporate the water than to maintain the same surface just above 0° C. Calculations show, however (ref. 23), that the total area that requires heating must also be considered in evaluating the total heat requirement. Therefore, the size of the component will generally influence which of the two methods of ice prevention is used.

The heat supplied to a component for icing protection (fig. 16) warms the impinging water to the component surface temperature and evaporates part or all of the impinging water. Some heat is lost to the ambient air

by convection. The relative magnitudes of the external heat losses shown in figure 16 are typical for anti-icing a wing surface and are shown as a function of surface distance aft of an airfoil leading edge. In addition, some of the heat is lost to adjacent structure by conduction. The external heat-transfer processes from a heated, wetted surface were postulated by J. K. Hardy (refs. 24 and 25). The processes were substantiated by in-flight data obtained by the staff of the NACA Ames laboratory (ref. 20). The Ames tests employed an aircraft with electrically heated dorsal wings (fig. 17). The electrically heated airfoils were instrumented with thermocouples (fig. 18) so that, with the conductivity and thickness of the material known, the internal heat loss could be calculated. Because of the thin outer skin, the chordwise heat conduction was considered negligible. Hence, the external local heat transfer was obtained from the total power input and the internal heat loss.

Typical results obtained from these studies are shown in figure 16. These data show that the heat for evaporating the impinging water and that lost to the ambient air by convection are approximately equal. The heat required to raise the impinging water to the surface temperature is only a small fraction of the total heat input. At the leading edge the heat flow is about 3900 Btu/(hr)(sq ft), while aft of the impingement area the local heat flow is 2400 Btu/(hr)(sq ft) or less.

In order to demonstrate that the results obtained in icing conditions in the tunnel were the same as those obtained in flight, a wing section carried on the C-46 aircraft during the Ames laboratory flight tests was also tested in the icing tunnel, and the data were compared (ref. 21). The results showed that in similar icing conditions, as determined by measurements of the cloud conditions by similar instruments, the data agreed satisfactorily.

For high-speed, high-altitude aircraft, the icing-protection heat requirements (due to changes in heat transfer and evaporation considera-tions influenced by speed and altitude) of a thermal anti-icing sytem are excessive. For example, calculations showed that the heat required for evaporating all the water impinging on a jet-powered transport exceeds 7,000,000 Btu/hr. Since this heat would be taken from the jet engines, a severe performance penalty would result (ref. 23).

In order to reduce the thermal requirements for airframe components, cyclic de-icing systems were studied. In cyclic de-icing, ice is per-mitted to form on the airplane surfaces and is then removed periodically by a short intense application of heat. During the heating period, the bond between the surface and the ice is melted and the ice is removed by aerodynamic forces. Only a few components or sections of a component are heated at a time, the rest being allowed to ice. Because the compo-nents are heated successively, proper grouping of the components permits shifting of heat from one group to another and thereby maintaining a con-stant heat load. The icing or heat-off time is determined by the amount of ice that can be tolerated on a component without seriously affecting its performance.

Numerous thermal cyclic de-icing systems were studied in the Lewis icing tunnel, typical of which was the hot-gas cyclically de-iced airfoil shown schematically in figure 19. The initial NACA design consisted of a conventional double skin, a two-way hot-gas supply duct with valves for cycling the hot gas into the plenum or D-duct running spanwise at the leading edge, and a conducting fin attached to the supply duct and airfoil skin at the leading edge near the stagnation region (ref. 26). A two-way gas-supply duct was used so that the hot gas would flow outboard and return in an adjoining rear passage in order to maintain a constantly hot supply line. The valves in the supply line open in spanwise sequence, thereby permitting a constant flow of gas in the forward passage and greatly avoiding thermal lags. Because the forward passage is continuously heated, the fin conducts heat to the skin at the stagnation region, thereby providing a narrow ice-free spanwise parting strip. This ice-free parting strip splits the ice cap that usually forms over the nose of the airfoil and facilitates ice removal by aerodynamic forces during the heating period.

The model was extensively instrumented with thermocouples in the skin and structural members and in the air passages in chordwise planes at several spanwise locations. Flow to the various sections was carefully metered by orifices in the air-supply lines. Timing of the fast-acting poppet-type cycle valves was made with electronic timers.

The results obtained from extensive studies of this model (refs. 26 and 27) show that savings in total heat input of as much as 75 to 90 percent of the heat required to prevent ice on the same wing were achieved. Similar results were obtained at both the NACA (ref. 28) and NAE facilities with electrically de-iced airfoils. Subsequent studies with a 36° swept wing (ref. 17) show that the tangential air-flow component along the span is sufficient to eliminate the need of a spanwise ice-free parting strip for facilitating removal of the ice formation. Systems similar to the NACA hot-air cyclic de-icing systems are currently being used by some manufacturers in the latest jet aircraft.

The use of a cyclic de-icing system necessitates an evaluation of the aerodynamic penalties associated with the ice formations permitted to build up during the unheated portion of a cycle (fig. 20). A number of airfoil models were tested to obtain the drag characteristics of cyclically de-iced airfoils in icing conditions (refs. 17 and 18). The results of these tests show that the drag and lift changes averaged over a cycle do not constitute a serious operational hazard if the length of the cycle can be adjusted to the serverity of the icing condition.

In addition to thermal de-icing systems, ice can be removed from most airfoil surfaces by a mechanical de-icing system consisting of a high-pressure pneumatic boot (fig. 21). In this system, inflatable tubes are sandwiched between two layers of rubber or neoprene. When ice forms on the outer surface of the boot, compressed air is bled periodically into the tubes which then inflate for a period of 3 to 6 seconds. Vacuum is

applied to the tubes to maintain the surface flush during the off part of the cycle. Studies in the icing tunnel show that these de-icers will effectively remove the main ice formations; however, the small flakes of residual ice adhering after the removal cycle will cause a section-drag increase of up to about 30 percent (unpublished data). Experimental studies indicate that removal of these residual ice formations by sublimation is a long process (ref. 29). These drag increases, therefore, can penalize aircraft performance over a much longer portion of the entire flight than for just the duration of the icing encounter.

The engine is the most vital component on the airplane requiring icing protection. Work on icing protection for engine air inlets and induction systems covered piston and jet engines. The work on piston engines, summarized in an NACA technical report (ref. 30), led to the recommendations incorporated in figure 22 for a typical arrangement of an engine induction system. Such a design includes (1) an air inlet, which reduces the intake of water and snow to a minimum by utilizing the inertia and momentum differences between air and water particles to separate the droplets out of the air at the inlet, (2) aerodynamically clean flow passages to prevent ice accretion on exposed parts, (3) air-metering devices located in a warm, dry region, (4) throttle and throttle bodies kept above freezing, and (5) fuel injected downstream of the heated surfaces to prevent fuel-evaporation icing. Aircraft that incorporate many of these features, including the inlet-type shown, are the Convair-240 and some versions of the Lockheed Constellation.

The high speeds of jet-powered aircraft and the large engine air flows necessitated a reappraisal of the icing problem for jet engines compared with that for the reciprocating engine. While the early centrifugal jet engines were not generally critical with respect to inlet and engine icing, because of engine geometry and structure, the axial-flow engines were adversely affected by icing. The icing of engine inlet guide vanes (refs. 31 to 33) and inlet screens constituted an icing hazard (fig. 23) that not only reduced the available thrust and increased specific fuel consumption but could cause engine failure. The icing hazard of a fixed inlet screen was aptly demonstrated by the simultaneous loss of eight F-84 aircraft over Indiana after a brief encounter with severe icing conditions in 1951. Tests in the Lewis icing tunnel also showed that the pressure loss associated with icing of guide vanes could cause large pressure losses and hence thrust losses (ref. 33). Several icing protection systems using alcohol or hot gas injection into the airstream to provide protection for the screen, accessory housing, and guide vanes were studied by NACA and NAE. With these systems, however, contamination of the compressor air (which is often used for cabin pressurization) or large thrust losses resulted.

The use of thermal icing protection for most engine components appeared most feasible. In the case of the screen, however, electro-thermal means did not appear attractive because of the large heating rates required.

Consequently, the complete elimination of the screen or retraction during
an icing encounter appeared mandatory. Elimination of the screen exposed
the engine to damage from ice chunks breaking off from unprotected compo-
nents ahead of the compressor and entering the engine. Practically all
types of axial-flow engines tested at the military services Mt. Washington
icing facility have suffered partial or complete engine failure from in-
gestion of such ice chunks. Thermal icing protection is required, there-
fore, for all components of the engine inlet that may shed these ice
chunks if left unprotected.

In the axial-flow engine the inlet guide vanes upstream of the com-
pressor ice quickly. Complete icing protection of these members is re-
quired if the engine is to function in icing conditions. A study of
means for heating the guide vanes internally with hot air was conducted
with a cascade of five vanes mounted in a rectangular duct set in the
icing tunnel (fig. 24). Ice collected on the leading and trailing edges
of the highly cambered blades used for inlet guide vanes. For this
reason, a saving of 50 percent of the heating air flow (fig. 25) is
achieved if the interior of the vane is partitioned to restrict this hot
air to the areas of the blade on which ice collects. This partitioning
of guide vanes has been adopted for some current engines.

Because the engine accessory dome collects ice that may break off
after reaching a destructive size and enter the engine, research was con-
ducted on the heating requirements for several jet-engine accessory domes.
An electrical icing protection system was used in order to obtain selec-
tive and controlled heating and thereby verify theoretical local heat-
transfer data (ref. 22 and unpublished data). The domes were tested also
with rotation to simulate turboprop installations in order to study the
effect of rotation on heating requirements. In general, the rotational
effect was negligible for the size models tested.

While it is apparent that aircraft operating at relatively low air-
speeds and at altitudes less than 20,000 feet will require airframe icing
protection equipment, high-speed, high-altitude aircraft, on the other
hand, may require little if any such equipment. These aircraft cruise at
altitudes where little or no icing occurs. Studies in high-speed icing
duct tunnels (refs. 34 to 36) show that icing can occur at speeds up to
a Mach number of approximately 1.3; however, because of aerodynamic heat-
ing of the surfaces at this high speed, such icing conditions would require
low air temperatures. The frequency of encountering severe icing at low
air temperatures on a statistical probability basis is almost negligible.
The icing problem for these aircraft, therefore, is confined primarily to
climb and let-down conditions. Because of their high rates of ascent and
descent, the icing encounters for these aircraft are of short duration.
Consequently, the flight plan and aircraft mission are becoming increas-
ingly more important in determining the necessity for airframe icing pro-
tection equipment.

A limited operational analysis of an interceptor and a transport air craft was presented in a paper by the author at an NACA conference on Some Problems of Aircraft Operation (Nov. 17-18, 1954). This study showed that thin-winged interceptor aircraft with a high rate of climb and descent and cruising at high altitude do not appear to require an airframe icing protection system except possibly during a landing operation. This study suggested that a partial or a simple one-shot icing protection system could be installed at minimum weight, structural, and performance penalty to cope with an icing encounter during landing. The study also concluded that jet transports, because of their slower rates of ascent and descent, should be provided with an airframe icing protection system. Since the engine is so vulnerable to ice damage, complete engine protection is required for both types of aircraft.

In summary, therefore, the NACA research programs have provided sufficient data or have established techniques whereby icing-protection requirements for most aircraft components can be determined sufficiently accurately for engineering purposes. The data obtained have been generalized whenever possible; however, it is recognized that certain specific installations at present still require testing in an icing tunnel or in flight. Meteorological studies are providing sufficient information on conditions conducive to icing on which to base the design requirements of aircraft components and to determine the need of icing protection for specific aircraft and flight plans. While this paper deals primarily with NACA studies in icing research, the contributions of other agencies including the groups operating at the Mt. Washington facilities, the U. S. military establishments, the U. S. aviation industry, the Canadian NAE, and other groups in the United States, Great Britain, and France must also be recognized. All these groups have cooperated and exchanged ideas that have aided in the successful solution of many icing problems.

APPENDIX A

ICING TUNNEL FACILITIES

The amount of time required for both aircraft and equipment main-
tenance to obtain sufficient data in flight toward the solution of icing
problems, together with the difficulty of obtaining data in specified,
controlled icing conditions, resulted in the design and construction of
an icing wind tunnel at the NACA Lewis laboratory in 1943-1944.

The Lewis icing tunnel is a single-return closed-throat tunnel, the
general arrangement of which is shown in figures 12 and 26. The tunnel
is constructed of steel plate and is insulated with a 3-inch thickness of
Fiberglas. The outer nonstructural shell covering the insulation is made
of 1/8-inch steel sheets.

The tunnel is anchored at each end of the test section and at each
end of the drive motor and supported by columns and sliding expansion
joints at all other points in order to allow movement due to temperature
stresses. The over-all size of the tunnel shell is about 198 feet long
and about 75 feet wide. The test section and a portion of the entrance
cone and diffuser are surrounded by a steel housing to provide space for
the essential test equipment and operating personnel. This space is
called the test chamber. Because the test section is vented to the chamber,
the air pressure decreases in the chamber during operation of the tunnel
(normally less than 3 in. Hg). An air lock is provided to permit access
by personnel to the chamber during a run.

The test chamber contains three floor levels: the ground floor, con-
taining electrical, thermocouple, water, and balance-scale equipment; the
second floor, containing the test section of the tunnel and the various
controls, manometers, recording instruments, and associated equipment;
and the third floor, containing auxiliary measuring equipment. Personnel
access to the tunnel is generally from the second floor of the test chamber,
while models are lowered into the test section from the third floor through
a removable 48- by 140-inch access hatch in the roof of the test section.

The test section is rectangular in shape, 9 feet wide, 6 feet high,
and 20 feet long. The air enters the test section from a large rectangu-
lar section giving a contraction ratio of about 14 to 1. The test section
of the tunnel is provided with a turntable on which models can be mounted,
as well as side-wall trunnion mounts. The maximum tunnel airspeed with
icing conditions and a large model in the test section is 260 knots.

Windows are provided on both sides and in the roof of the tunnel
test section to allow observation of models during a test. The windows
in the tunnel sides are laminated, electrically heated units similar to

windshields on many aircraft, while the windows in the test section roof are unheated. The power supplied to new windows currently being installed is 500 watts per square foot. The temperature of the plastic inner layer of the window is detected by a nickel wire element. This element is used in a bridge circuit to control the window temperature.

Turning vanes are used in all right-angle corners of the tunnel. The vanes downstream of the test section and ahead of the drive fan are steam-heated to prevent icing.

The drive motor for the tunnel develops 4160 horsepower. The drive consists of a doubly fed wound-rotor induction motor. Power is supplied directly to the stator, while the power for the rotor is supplied by a four-machine variable and fixed frequency setup. A variable-speed d-c motor, driven according to the Ward-Leonard system, drives an a-c genera-tor. The generator supplies the power to the tunnel drive-motor rotor. The speed of the drive motor is governed by the speed of the a-c genera-tor or d-c motor, the speed of these machines being controlled by varying the voltage to the d-c motor. The drive motor has a speed range from 0 to 540 rpm. A 200,000-cubic-foot-per-minute, 50-horsepower blower is used to cool the drive motor.

The tunnel drive motor is coupled directly to a 25-foot-diameter drive fan with 12 blades. The fan blades are wooden, with the leading edges of the blades protected by neoprene abrasion shoes. Stationary contra-vanes are used ahead of the fan.

A ventilating tower is located downstream of the drive motor. This tower permits an exchange of tunnel air with outside air. The primary use of this unit has been to provide an additional cooling load to help regulate the tunnel air temperature for certain test conditions. In ad-dition, a finned-tube heat exchanger with a capacity of 5,000,000 Btu per hour is available to aid in regulating the tunnel air temperature.

A compression-type refrigeration system located in a nearby building is used to cool the tunnel air to the required icing condition. The tunnel is cooled by passing the air over a bank of refrigerated finned heat ex-changers located in an area between the drive motor and the tunnel spray system. The total refrigeration capacity is about 7700 tons. The normal cooling load for the icing tunnel requires from 1200 to 2100 tons; however, this requirement varies with climatic conditions. Air temperatures as low as -40° C can be obtained, although most tests are conducted in the range of -3° to -20° C.

Icing conditions similar to those encountered in the atmosphere are created by a battery of air-water atomizing nozzles. A view of the spray system looking downstream into the test section is shown in figure 13. The spray nozzles are mounted in six horizontal spray bars and located to

give a uniform cloud approximately 4- by 4-feet in the test section.
Controls for the spray system are located in airfoil-shaped enclosures
at one end of each strut.

A sketch of the air-water atomizing nozzles used in the spray system
is shown in figure 27. The nozzle assembly consists of air and water
supply lines, steam line to prevent icing of the entire strut, and the
spray nozzle (Inconel). Approximately 80 nozzles are used to obtain an
adequate cloud in the tunnel. The nozzles were specially developed for
the tunnel to yield droplet sizes ranging from a mean effective size of
4 microns at low water flows to about 20 microns at maximum water flows.
Air pressures of 60 to 80 pounds per square inch are used normally to
atomize the water, while the water pressures range from a few pounds
above the air-pressure values up to 140 pounds per square inch. The
large water-pressure values correspond to large water flows and large
droplet sizes. The droplets produced by these nozzles are not unifrom
in size but vary approximately in accordance with a Langmuir D or E
drop-size distribution (ref. 37). For a constant water flow, the liquid-
water content in the tunnel varies with the airspeed. In addition, the
contraction of the tunnel entrance cone affects the droplet paths and
local water concentration in the tunnel. Consequently, maximum or mini-
mum values of water content and droplet size independent of tunnel air-
speed cannot be stated explicitly.

The water used for the spray system passes through a 500-gallon-per-
hour-capacity demineralizer. The demineralizer consists of two anion and
cation filter beds that remove all minerals from the water, thereby pre-
venting fouling and plugging of the spray system. From the demineralizer,
the water is piped into a storage tank with a capacity of 750 gallons.
The storage tank is kept full by a float switch that turns the demineraliz-
er on and off to maintain a given water level in the storage tank. From
the storage tank the water is piped to two turbine water pumps with a
capacity of 5 gallons per minute each at 150 pounds per square inch gage.
The water is pumped through three rotameters for flow measurement and then
into a steam heat exchanger that heats the water to a temperature of 80°
to 90° C. Heating of the water is necessary to prevent freeze-out of the
water when it is air-atomized to cloud droplets in the tunnel. Following
the heat exchanger the water is filtered at each strut control box. The
water pressure is regulated at each strut by a pressure regulator con-
trolled by the tunnel operator. The water pressure is sensed by a pres-
sure transmitter, which changes water pressure to pneumatic pressure. The
water pressures in each spray strut (in the form of pneumatic pressure)
are indicated on a manometer board in the test chamber.

Air is furnished to the water-spray system from a service air line
with a capacity of 6 pounds per second at 120 pounds per square inch.
This air is passed through a pressure regulator, a steam heat exchanger
(which heats the air to approximately 80° to 90° C), and a two-stage
filter before entering the strut control boxes. The air pressure is
also controlled from the test-chamber control area.

A separate spray system consisting of 4 to 9 nozzles is used to inject dyed water into the tunnel for experimental studies of droplet impingement characteristics of various bodies (ref. 15).

A balance frame is provided with a 6-component force-measuring scale system. Data are recorded automatically on tapes at each balance. Electrically heated co-axial pressure tubes are used to obtain pressure data. All pressure data are recorded photographically from multi-tube manometer boards. Temperature data obtained with copper-constantan thermocouples are recorded on automatic flight recorders. The control equipment includes variable transformers for power control to models, automatic temperature controller for heated air to models, and various recording instruments for heat-source control. Standard instruments are used to record tunnel airspeed and air temperature. An NACA pressure-type icing-rate meter is used to measure the liquid-water content of the tunnel atmosphere. Special instrumentation is added whenever required for a particular study.

Heated air for providing models with icing protection is supplied by three heat exchangers. The air from these exchangers is heated by the exhaust from a jet-engine combustion can. Each heat exchanger has a flow capacity of 1000 pounds per hour with pressure regulation up to 120 pounds per square inch. Orifices in each line allow a measurement of the flow from each exchanger. Constant air temperature over a wide range of air flows is obtained by an automatic flow control that regulates the amount of cold air permitted to mix with heated air from the exchangers.

Electric heating supplied to models for icing protection can be obtained from either a-c or d-c sources; however, a-c is generally preferred. The d-c system capacity is 28 volts and rated at 100 amperes. In addition, a 12-volt d-c system rated at 50 amperes is also available. A 29-volt a-c system rated at 50 amperes is available and is used for heater studies for which the heater load is normally run on d.c. A 110-volt single-phase system and a 208-volt, three-phase, 50-ampere system are available for large electrical loads. Selective power inputs (a-c three-phase system) to electrically heated models are metered (power recorded on a recording wattmeter) by means of 18 variable transformers rated at 3 amperes, 16 variable transformers rated at 9 amperes, and 3 variable transformers rated at 45 amperes. A 400-cycle inverter capable of supplying 1500 volt-amperes at 115 volts is also used for some instrument tests.

Electronic timers are available by which specified heating and icing periods for either electric or air heating systems can be controlled.

The 136-inch-high multi-tube manometer board is so arranged that it may operate as an integrating type or a standard board. A total of 298 readings can be obtained from the board. Additional U-tube and standard manometer boards are available as required. Most of the tubes are also connected to an air-purge system by which air is bled through the tubes

back to the model. An air-operated cylinder or pincher closes off the tubes at the manometer to prevent the purge air from blowing the manometer fluid out of the bonds. The purge air prevents the entry of water from the spray cloud into the tubes and blocking or freezing of the unheated portions of the pressure lines. During this purging procedure, no manometer-board readings are taken.

For aerodynamic studies of airfoils in icing conditions, the airfoil surfaces aft of the region protected by the icing protection system (called afterbody) are generally heated. This heating is required, since the turbulence level and supersaturated air in the test section cause a frost deposit on the cold portions of a model. These deposits have rarely been observed in natural flight icing. Such frost deposits increase the measured model drag. A steam line operating at +5 to -3 inches of mercury is used to heat these afterbodies. To avoid steam leakage from the model into the tunnel, the afterbody is operated at a negative pressure by means of a small ejector and a barometric condensor located externally of the model.

Photographs of ice formations during a test are obtained with high-speed electronic flash equipment, while conventional camera equipment is used for pictures taken in the tunnel at the conclusion of a test. Color photography has proved to be the most satisfactory for movie film recording of data in the presence of the spray cloud.

Airfoil models normally span the vertical height of the tunnel. Chords of these models have ranged from 13 to 96 inches or larger. Horizontal model mounting has also been used occasionally; however, because of wind-tunnel-wall interference effects, the vertical mounting is preferred. Bodies of revolution and inlets tested are normally less than 36 inches in diameter.

In addition to the 6- by 9-foot icing tunnel, two smaller high-speed icing-duct tunnel facilities are also used. Techniques equivalent to those just described are used in these tunnels. A schematic diagram of the 3.84- by 10-inch tunnel presented in figure 28 shows the inlet diffuser section with screens, the plenum chamber with flow-straightening tubes, the bellmouth tunnel entry, the test section, and the outlet diffuser section. The tunnel is designed to provide a range of subsonic Mach numbers from 0.3 to 0.8 and a supersonic Mach number of 2.0. Altitudes up to 30,000 feet may be simulated.

A supply of refrigerated air initially at approximately -20° F and with a specific humidity of 5.0×10^{-4} pound of water per pound of dry air is conditioned to provide the desired temperatures and humidities at the tunnel test section. The humidity of the airstream is controlled by means of steam injected at a point sufficiently far upstream to ensure thorough mixing at the tunnel entry.

One wall of the tunnel contains a large glass section for observation and visual measurements. The other wall has five portholes for access to the inside of the tunnel and removable plugs for installation of instrumentation at various stations along the tunnel. Permanent instrumentation of the tunnel at the test section includes static-pressure taps along the top and bottom surfaces of the tunnel and pressure taps and thermocouples in the plenum chamber.

A schematic diagram of the component parts of a 12- by 12-inch icing duct tunnel is shown in figure 29. The tunnel characteristics are in general similar to the 3.84- by 10-inch tunnel. Subsonic speeds up to a Mach number of 0.75 can be achieved with small airfoil models. For icing studies the airspeed is maintained in the subsonic and low supersonic speed ranges.

APPENDIX B

OPERATIONAL TECHNIQUES

The following are techniques used for model testing in the Lewis icing tunnel and associated facilities.

Thermocouple Installations

Whenever possible, all skin or surface thermocouples (copper-constantan) are peened into small holes drilled into the surface as shown in figure 30. The ball at the junction of the thermocouple is just large enough to fit into the hole, so that peening the surface around the ball will result in a firmly anchored thermocouple. The ball should be as close to the outer surface of the skin as possible. For very thin metal skins (0.005-inch stainless steel, e.g.) spot-welding the thermocouple on the inner surface of the skin is acceptable. The thermocouple leads should not be secured on the outer surface of the model, since ice will anchor on the leads. If splicing of thermocouple leads is required, such splices should be made in a protected, constant-temperature location, outside the model in the test chamber. All thermocouple leads should be protected against moisture; asbestos-covered wires are not generally recommended for models in icing conditions. Shielded thermocouples are recommended for obtaining measurements of hot air temperature, although a trailing thermocouple such as that shown in figure 30(b) is acceptable.

Tunnel Air Temperature

The tunnel air temperature is obtained with a probe that separates the entrained water from the airstream as shown in figure 31. The probe consists of a nose and rear cap and a housing containing a temperature-sensing element. Holes are located in the housing so that the air flows through the probe from the rear to the front of the probe. The locations of these holes are based on pressure-distribution studies. The water droplets, because of their inertia, do not enter the housing at the rear locations. Because the nose-cap diameter is larger than the housing diameter, the housing is protected from icing. The nose cap is allowed to ice. Thermal icing protection could be incorporated in the nose cap; however, an error in the indicated temperature would be incurred. The average temperature-recovery factor for these probes is about 84 percent and is constant over a range of Mach numbers from 0.2 to 1.0. In the NACA icing tunnel the probes are used to measure air temperature in the low-speed section upstream of the spray system and ahead of the contraction cone. The air temperature measured by these probes is therefore essentially a total air temperature. Because the tunnel is always at

least saturated when the spray system is used, the ambient-air tempera-
ture in the test section is computed by conventional wet-air equations
(ref. 21). The total air temperature measured in the low-speed section
of the tunnel is used for a base in these calculations.

Temperatures from Rotating Bodies.

A typical means used to transmit the temperatures from a rotating
body to a recorder is shown schematically in figure 32. The thermocouple
leads from the body are fed through a hollow motor shaft to the rear of a
motor housing and through a thermocouple selector switch into a steam-
filled jacket that rotates with the shaft. From the rotating jacket,
copper leads are attached to a slip-ring and brush assembly. From this
assembly, copper leads are again led into a steam-filled stationary
jacket. Copper-constantan leads are used from the stationary jacket to
a thermocouple selector unit and to a flight recorder. The steam jacket
is used to provide a constant temperature at critical junctions in the
thermocouple circuit, where the wire metal in the thermocouple leads is
changed from copper and constantan to all copper and back again.

Pressure Tubes

In icing conditions all pressure tubes subject to water impingement
(pitot-static tubes, tubes in survey rakes and in the boundary layer, etc)
must be protected against icing. In the Lewis icing tunnel such pressure
tubes are generally electrically heated. A co-axial tube is used consist-
ing of two concentric tubes separated by a woven glass sleeving insulation
(fig. 33). The ends of the tubes exposed to the airstream are silver-
soldered and shaped to obtain either static or total-pressure tubes. Tube
sizes of 0.093- to 0.437-inch outside diameter and 0.057- to 0.393-inch
inside diameter with wall thicknesses of 0.005 inch are in common usage.
These tubes are made of Inconel. A special tube bender was developed by
NACA personnel to avoid collapsing of the co-axial tubing during bending
of the tubes to a desired shape.

Surface Pressure from Rotating Body

A scheme similar to that used to obtain temperatures from rotating
bodies is also used to obtain surface pressure measurements. Pressure
lines from a model are fed into a hollow shaft (fig. 34). Each tube is
then allowed to vent into a chamber composed of the hollow shaft, bear-
ings, and a stationary housing. All pressure sealing is accomplished by
the bearings and felt seals. The pressure from each sealed chamber is then
transmitted to a manometer. A water-jacket cooling system (not shown) is
provided for high-rotational-speed operation. This pressure system permits
simultaneous readings of many pressures and is generally limited only by the
number of bearings used.

APPENDIX C

ICING INSTRUMENTS

The determination of liquid-water content and droplet-size distribution of natural and artificial clouds has received considerable attention in connection with cloud physics studies and, in particular, in aircraft icing studies. A knowledge of the liquid-water content and droplet-size distribution in clouds is of fundamental importance in evaluating rate and area of ice formation on various aircraft components, rate and area of erosion by impinging droplets on various aircraft surfaces such as radomes, reduction of visibility, attenuation of radar, and the basic mechanism of cloud formation and precipitation.

Numerous methods for determining these parameters have been proposed and tested, but each method suffers limitations as to accuracy or ease in obtaining or reducing the data to useful form. In some cases the limitations become very severe when measurements are attempted in high-speed airstreams. In addition to the rotating multicylinders and pressure-type icing-rate meter discussed in the test, some methods and techniques that have been widely employed to determine liquid-water content and/or droplet size are:

(1) Cloud camera
(2) Oil slides
(3) Oil-stream aeroscope
(4) Heated probes

The methods are described and discussed in references 38 to 40.

The use of cameras (fig. 35) to photograph droplets directly in a cloud (ref. 38) is based on fundamental principles and is basically a sound technique, but there are practical difficulties. Because of the high magnification required, the volume of the field of view is extremely small. As a result, the average number of droplets per 8- by 10-inch picture is small in clouds of moderate liquid-water contents. Therefore, a large number of pictures are required in order to obtain a size distribution. Since the magnification required is high, it is difficult to design a camera so that the object plane is outside the undisturbed airstream about an airplane or camera mount.

The oiled-slide technique, where a glass slide covered with a suitable oil is exposed to a droplet-laden airstream and is then photographed through a microscope, has been used also to determine droplet-size distributions. This method yields photographs with a large number of droplets per picture from which the droplet sizes may be measured. However, because of the relatively large size of the slide compared with the size of droplets, the over-all collection efficiency and the local collection efficiencies

of the slide vary considerably with droplet size. The droplet-size distribution for any given area of the slide must be corrected according to the local collection efficiencies in order to obtain the true droplet-size distribution of the cloud. The local collection efficiencies used for this correction are based upon that of a ribbon in ideal two-dimensional flow. The exposure time required in order not to saturate the slide with droplets must be of the order of a fraction of a second. This presents some difficulties, in that the slide must be moved rapidly or a protective cover must be opened and closed rapidly. This motion disturbs the airflow field in the vicinity of the slide, and therefore the collection efficiencies of the slide are not the same as for a ribbon in ideal flow.

An oil-stream aeroscope composed of five main parts (fig. 36) - droplet pickup probe, circulating pumps for oil and air, photographic cell, light source, and a photomicrographic camera - has been developed. The droplet pickup probe consists of a small-diameter tube with a small hole on one side. When operating, the probe is arranged so that the small hole faces upstream to the air flow carrying the cloud droplets. Oil is forced by a pump through the pickup probe in the direction indicated in the sketch. As the oil passes the small hole, any water droplets that enter are trapped in the oil. Oil does not flow out of the droplet pickup hole, because the oil pressure is maintained at atmospheric pressure by the air pump shown in figure 36. The oil containing the droplets then flows through the transparent plastic cell where the droplets are photographed with a photomicrographic camera. The channel through the plastic cell narrows down at the point where the pictures are taken, so that all the droplets are approximately in the object plane of the camera. After leaving the plastic cell, the oil passes through a filter and trap where the water droplets are removed. The droplet size and distribution can then be determined by measuring the images on the photographs from the known magnification. After the droplet distribution is known, the liquid-water content of the cloud can be calculated from the known geometry of the instrument, the airspeed, and the oil-flow rate. Limited data indicate that this instrument shows excellent promise for obtaining the desired information.

The heated-wire instrument consists basically of a loop of resistance wire (refs. 39 and 40) which is mounted in the airstream (fig. 37) and is heated electrically by passing current through the wire. The wire diameter is 0.021 to 0.064 inch, with a maximum power input of 31 to 300 watts, respectively (ref. 40). The change in wire resistance from the clear-air condition, resulting from cooling due to evaporation of impinging cloud water droplets, is used as a measure of the liquid-water content, or icing severity. Although the heated-wire instrument has several disadvantages as pointed out in reference 40, a workable instrument can be obtained that is very useful in studying cloud microstructure.

A variation of the heated-wire instrument is currently under development at the NACA Lewis laboratory. This instruments consists of a heated tube

operating at constant surface temperature with a variable power input. This instrument has the following advantages over a constant-power heated-wire probe:

 (1) The measured change in required power is linear with water impingement, because the surface temperature is fixed.
 (2) The change of heat-transfer coefficient under all conditions is minimized.
 (3) The sensitivity to water impingement is maximized.
 (4) The power input is easily measured.
 (5) With proper design, the time constant is less that that of a wire heated with constant power.

While the control circuit for this probe has proved formidable, a satisfactory unit has been designed and operated. The probe is currently being calibrated in the Lewis icing tunnel.

REFERENCES

1. Hacker, Paul T., and Dorsch, Robert G.: A Summary of Meteorological
   Conditions Associated with Aircraft Icing and a Proposed Method of
   Selecting Design Criterions for Ice-Protection Equipment. NACA TN
   2569, 1951.

2. Lewis, William, and Bergrun, Norman R.: A Probability Analysis of the
   Meteorological Factors Conducive to Aircraft Icing in the United
   States. NACA TN 2738, 1952.

3. Jones, Alun R., and Lewis, William: Recommended Values of Meteorologi-
   cal Factors to be Considered in the Design of Aircraft Ice-Prevention
   Equipment. NACA TN 1855, 1949.

4. Lewis, William, Perkins, Porter J., and Brun, Rinaldo J.: Procedure
   for Measuring Liquid-Water Content and Droplet Sizes in Super-
   cooled Clouds by Rotating Multicylinder Method. NACA RM E53D23, 1953.

5. Perkins, Porter J., McCullough, Stuart, and Lewis, Ralph D.: A Sim-
   plified Instrument for Recording and Indicating Frequency and Inten-
   sity of Icing Conditions Encountered in Flight. NACA RM E51E16, 1951.

6. Brun, Rinaldo J., Gallagher, Helen M., and Vogt, Dorothea E.: Impinge-
   ment of Water Droplets on NACA 65A004 Airfoil and Effect of Change in
   Airfoil Thickness from 12 to 4 Percent at 4° Angle of Attack. NACA
   TN 3047, 1953.

7. Brun, Rinaldo J., Gallagher, Helen M., and Vogt, Dorothea E.: Impinge-
   ment of Water Droplets on NACA 65_1-208 and 65_1-212 Airfoils at 4°
   Angle of Attack. NACA TN 2952, 1953.

8. Guibert, A. G., Janssen, E., and Robbins, W. M.: Determination of Rate,
   Area, and Distribution of Impingement of Waterdrops on Various Airfoils
   from Trajectories Obtained on the Differential Analyzer. NACA RM 9A05,
   1949.

9. Brun, Rinaldo J., Gallagher, Helen M., and Vogt, Dorothea E.: Impinge-
   ment of Water Droplets on NACA 65A004 Airfoil at 8° Angle of Attack.
   NACA TN 3155, 1954.

10. Brun, Rinaldo J., Serafini, John S., and Gallagher, Helen M.: Impinge-
    ment of Cloud Droplets on Aerodynamic Bodies as Affected by Compressi-
    bility of Air Flow Around the Body. NACA TN 2903, 1953.

11. Dorsch, Robert G., and Brun, Rinaldo J.: A Method for Determining
    Cloud-Droplet Impingement on Swept Wings. NACA TN 2931, 1953.

12. Brun, Rinaldo J., and Dorsch, Robert G.: Impingement of Water Droplets on an Ellipsoid with Fineness Ratio 10 in Axisymmetric Flow. NACA TN 3147, 1954.

13. Dorsch, Robert G., Brun, Rinaldo J., and Gregg, John L.: Impingement of Water Droplets on an Ellipsoid with Fineness Ratio 5 in Axisymmetric Flow. NACA TN 3099, 1954.

14. Brun, Rinaldo J., and Mergler, Harry W.: Impingement of Water Droplets on a Cylinder in an Incompressible Flow Field and Evaluation of Rotating Multicylinder Method for Measurement of Droplet-Size Distribution, Volume-Median Droplet Size, and Liquid-Water Content in Clouds. NACA TN 2904, 1953.

15. von Glahn, Uwe H., Gelder, Thomas F., and Smyers, William H., Jr.: A Dye-Tracer Technique for Experimentally Obtaining Impingement Characteristics of Arbitrary Bodies and a Method for Determining Droplet Size Distribution. NACA TN 3338, 1955.

16. Sherman, P., Klein, J. S., and Tribus, M.: Determination of Drop Trajectories by Means of an Extension of Stokes' Law. Eng. Res. Inst., Univ. Mich., Apr. 1952. (Air Res. and Dev. Command, USAF, Contract AF 18(600)-51, Proj. M992-D.)

17. von Glahn, Uwe H., and Gray, Vernon H.: Effect of Ice Formations on Section Drag of Swept NACA 63A-009 Airfoil with Partial-Span Leading-Edge Slat for Various Modes of Thermal Ice Protection. NACA RM E53J30, 1954.

18. Gray, Vernon H., and von Glahn, Uwe H.: Effect of Ice and Frost Formations on Drag of NACA 65_1-212 Airfoil for Various Modes of Thermal Ice Protection. NACA TN 2962, 1953.

19. Lewis, James P., and Blade, Robert J.: Experimental Investigation of Radome Icing and Icing Protection. NACA TM E52J31, 1953.

20. Neel, Carr B., Jr., Bergrun, Norman R., Jukoff, David, and Schlaff, Bernard A.: The Calculation of the Heat Required for Wing Thermal Ice Prevention in Specified Icing Conditions. NACA TN 1472, 1947.

21. Gelder, Thomas F., and Lewis, James P.: Comparison of Heat Transfer from Airfoil in Natural and Simulated Icing Conditions. NACA TN 2480, 1951.

22. von Glahn, U.: Preliminary Results of Heat Transfer from a Stationary and Rotating Ellipsoidal Spinner. NACA RM E53F02, 1953.

23. Gelder, Thomas F., Lewis, James P., and Koutz, Stanley L.: Icing Protection for a Turbojet Transport Airplane: Heating Requirements, Methods of Protection, and Performance Penalties. NACA TN 2866, 1953.

24. Hardy, J. K.: Kinetic Temperature of Wet Surfaces - A Method of Calculating the Amount of Alcohol Required to Prevent Ice, and the Derivation of the Psychrometric Equation. NACA WR A-8, 1945. (Supersedes NACA ARR 5G13.)

25. Hardy, J. K.: An Analysis of the Dissipation of Heat in Conditions of Icing from a Section of the Wing of the C-46 Airplane. NACA Rep. 831, 1945. (Supersedes NACA ARR 4I11a.)

26. Gray, V. H., Bowden, D. T., and von Glahn, U.: Preliminary Results of Cyclical De-Icing of a Gas-Heated Airfoil. NACA RM E51J29, 1952.

27. Gray, Vernon H., and Bowden, Dean T.: Comparison of Several Methods of Cyclic De-Icing of a Gas-Heated Airfoil. NACA RM E53C27, 1953.

28. Lewis, James P., and Bowden, Dean T.: Preliminary Investigation of Cyclic De-Icing of an Airfoil Using an External Electric Heater. NACA RM E51J30, 1952.

29. Coles, Willard D., and Ruggeri, Robert S.: Experimental Investigation of Sublimation of Ice at Subsonic and Supersonic Speeds and Its Relation to Heat Transfer. NACA TN 3104, 1954.

30. Coles, Willard, Rollin, Vern G., and Mulholland, Donald R.: Icing-Protection Requirements for Reciprocating-Engine Induction Systems. NACA Rep. 982, 1950. (Supersedes NACA TN 1993.)

31. Acker, Loren W.: Natural Icing of an Axial-Flow Turbojet Engine in Flight for a Single Icing Condition. NACA RM E8F01a, 1948.

32. Acker, Loren W.: Preliminary Results of Natural Icing of an Axial-Flow Turbojet Engine. NACA RM E8C18, 1948.

33. Gray, Vernon H., and Bowden, Dean T.: Icing Characteristics and Anti-Icing Heat Requirements for Hollow and Internally Modified Gas-Heated Inlet Guide Vanes. NACA RM E50I08, 1950.

34. Callaghan, Edmund E., and Serafini, John S.: A Method for Rapid Determination of the Icing Limit of a Body in Terms of the Stream Conditions. NACA TN 2914, 1953.

35. Callaghan, Edmund E., and Serafini, John S.: Analytical Investigation of Icing Limit for Diamond-Shaped Airfoil in Transonic and Supersonic Flow. NACA TN 2861, 1953.

36. Coles, Willard D.: Icing Limit and Wet-Surface Temperature Variation for Two Airfoil Shapes under Simulated High-Speed Flight Conditions. NACA TN 3396, 1955.

37. Langmuir, Irving, and Blodgett, Katherine B.: A Mathematical Investigation of Water Droplet Trajectories. Tech. Rep. No. 5418, Air Materiel Command, AAF, Feb. 19, 1946. (Contract No. W-33-038-ac-9151 with General Electric Co.)

38. McCullough, Stuart, and Perkins, Porter J.: Flight Camera for Photographing Cloud Droplets in Natural Suspension in the Atmosphere. NACA RM E50K01a, 1951.

39. Neel, Carr B., Jr., and Steinmetz, Charles P.: The Calculated and Measured Performance Characteristics of a Heated-Wire Liquid-Water-Content Meter for Measuring Icing Severity. NACA TN 2615, 1952.

40. Neel, Carr B.: A Heated-Wire Liquid-Water Content Instrument and Results of Initial Flight Test in Icing Conditions. NACA RM A54I23, 1955.

SEVERE ICING OF AIRCRAFT COMPONENTS

LEADING EDGE ICE FORMATION

COMPRESSOR INLET ICING

CARBURETOR SCREEN ICING
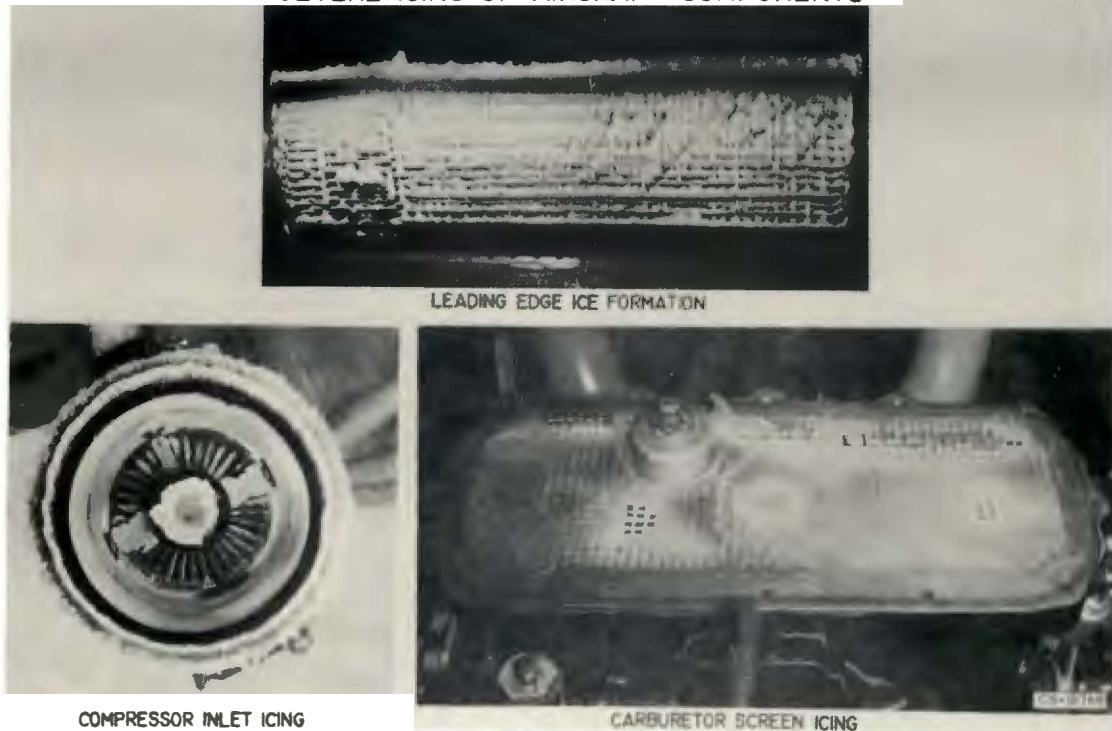
Figure 1.

AIRCRAFT SURFACES REQUIRING ICING PROTECTION

CS-10777
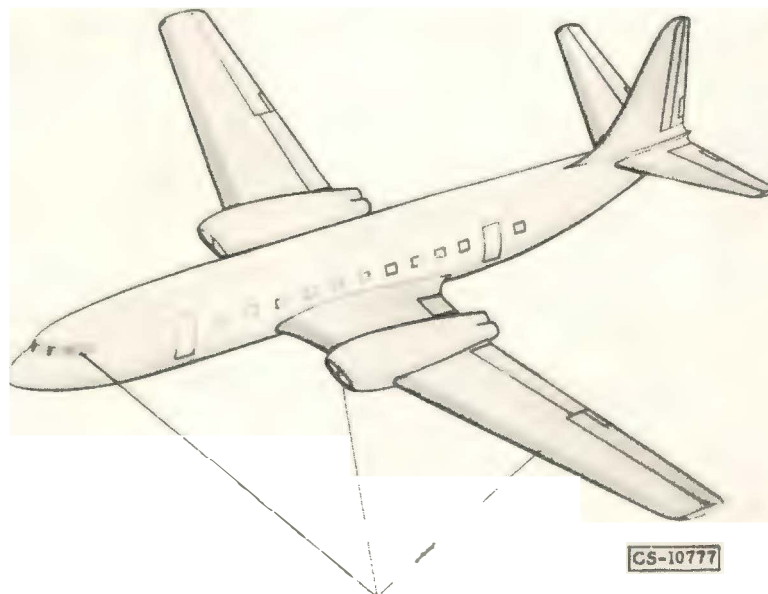
SHADING INDICATES AREAS
SUBJECT TO ICING

Figure 2.

DROPLET TRAJECTORIES ABOUT AIRFOIL

AIR STREAMLINES

DROPLET PATHS

[CS-10778]

Figure 3.

MULTI-CYLINDERS INSTALLED ON AIRCRAFT
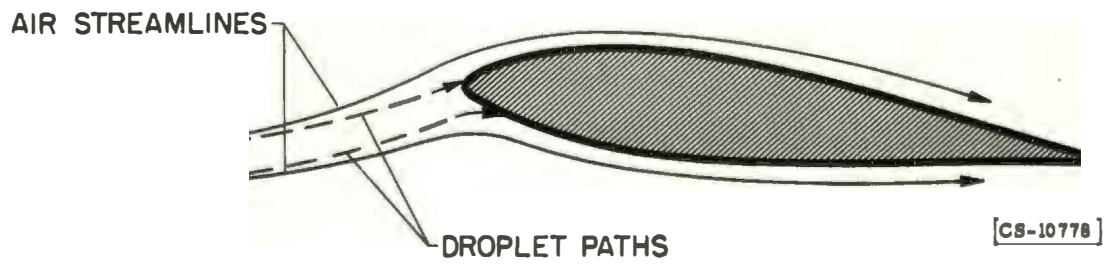
[CS-10761]

Figure 4.

PRESSURE-TYPE ICING RATE METER
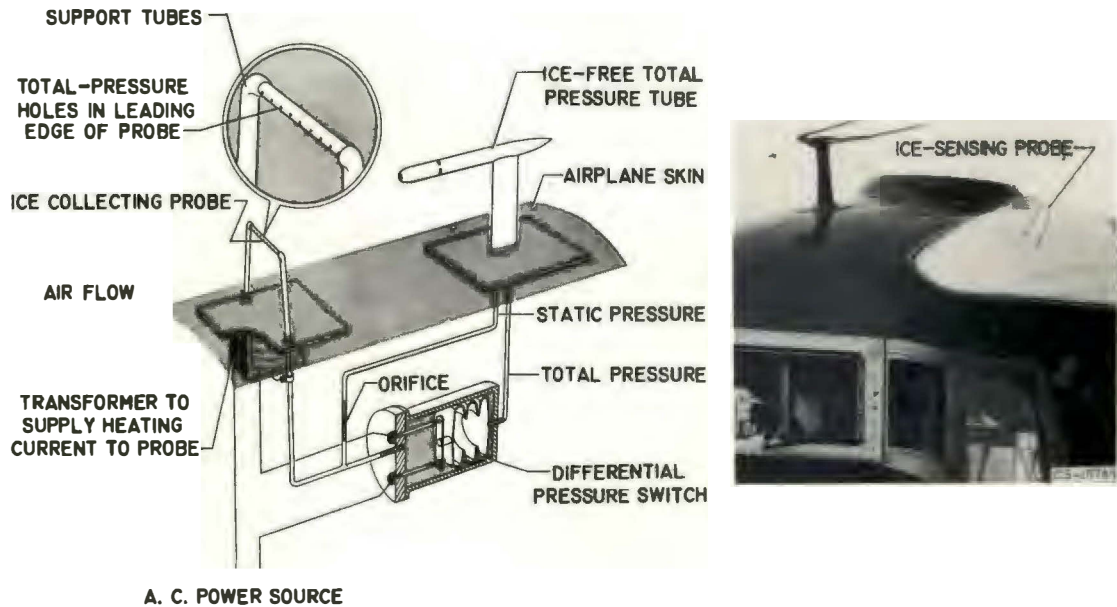
Figure 5.

WORLD ICING SURVEY ROUTES
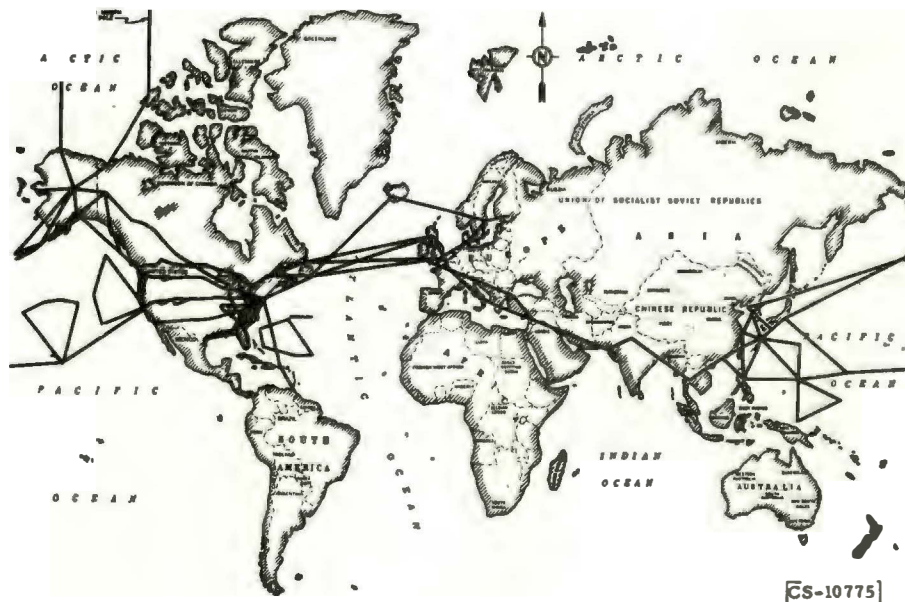
Figure 6.

WATER-DROPLET-TRAJECTORY ANALOG
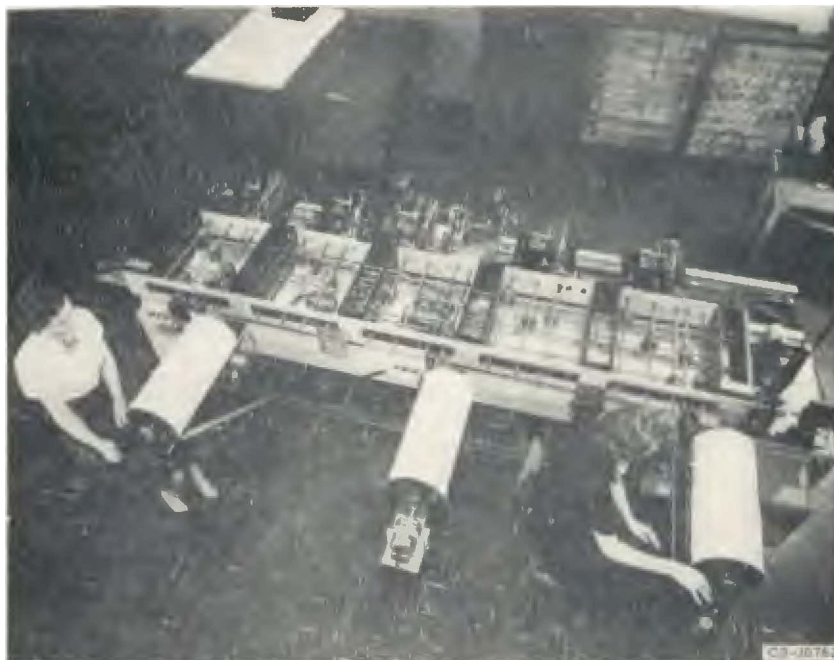
Figure 7.

LOCAL IMPINGEMENT RATES ON A 15-PERCENT THICK
SYMMETRICAL AIRFOIL

ANGLE OF ATTACK, 0°; WATER CONTENT, 0.7 GM/CU. M.
AIRSPEED, 150 KNOTS; CHORD, 8 FT

AVERAGE
DROP SIZE

15

8

LOCA WATER IMPINGEMENT RATE
LB/HR, SQ FT

SURFACE DISTANCE MEASURED FROM LEADING EDGE/CHORD

CS-10816

Figure 8.

MODEL USED IN OBTAINING EXPERIMENTAL IMPINGEMENT DATA
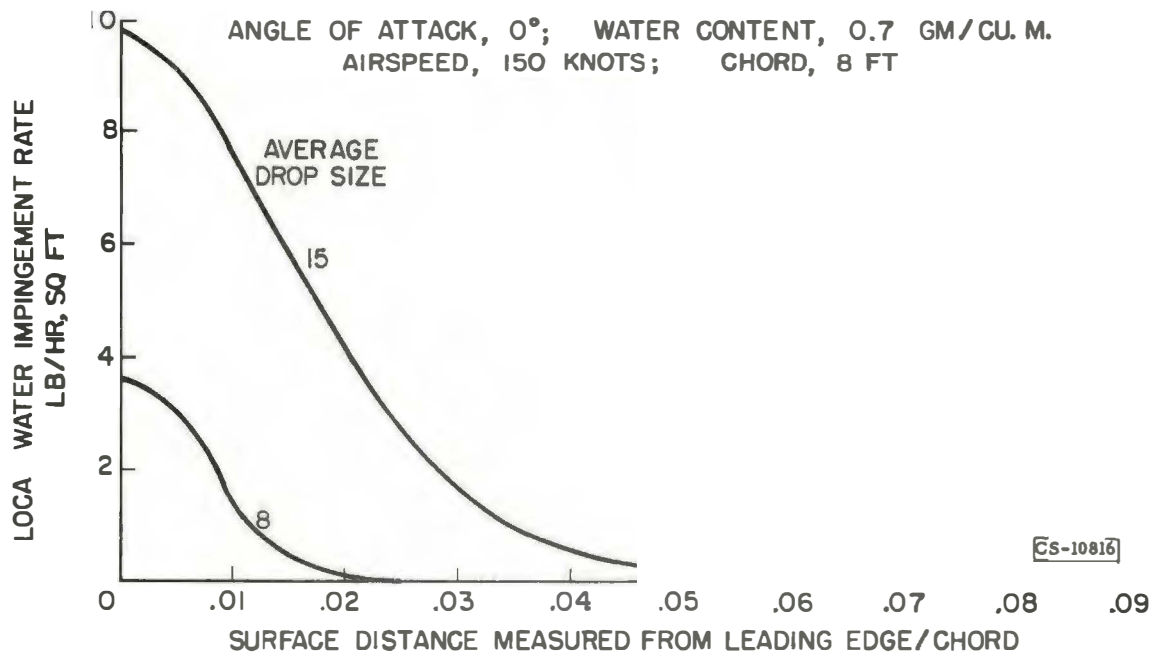
Figure 9.

COMPARISON OF THEORETICAL AND EXPERIMENTAL IMPINGEMENT DATA
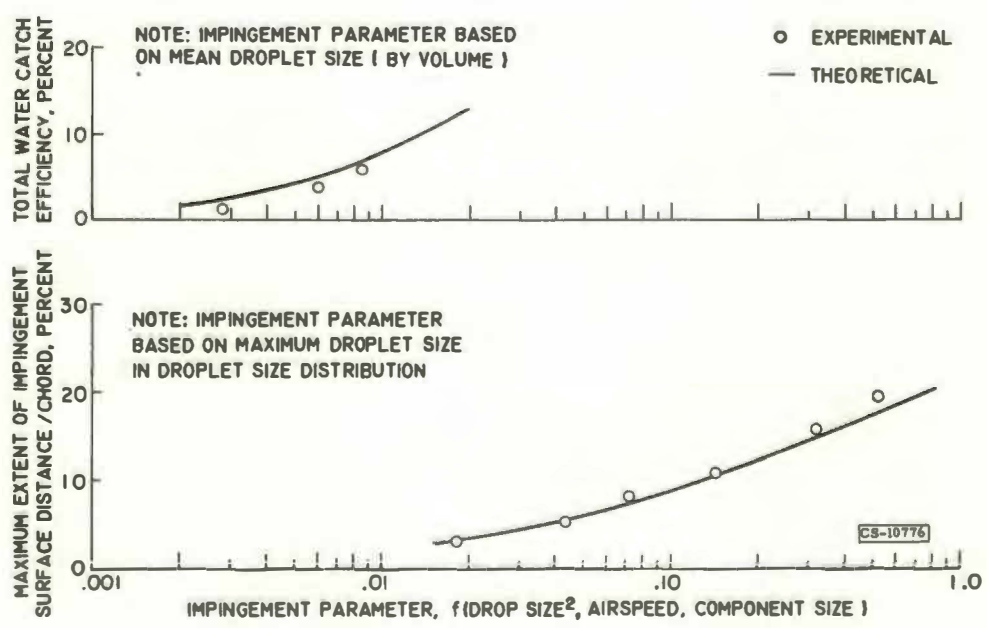
Figure 10.

TYPICAL AIRFOIL ICE FORMATIONS

CS-10766
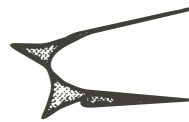
(A) RIME ICE. DATUM
AIR TEMPERATURE, 0° F

(B) DOUBLE PEAK GLAZE ICE.
DATUM AIR TEMPERATURE,
30° F. HIGH RATE OF WATER CATCH

Figure 11.

PLAN VIEW OF ICING TUNNEL

VENTILATING TOWERS

DRIVE FAN

REFRIGERATION COILS

HEAT EXCHANGER

TEST SECTION
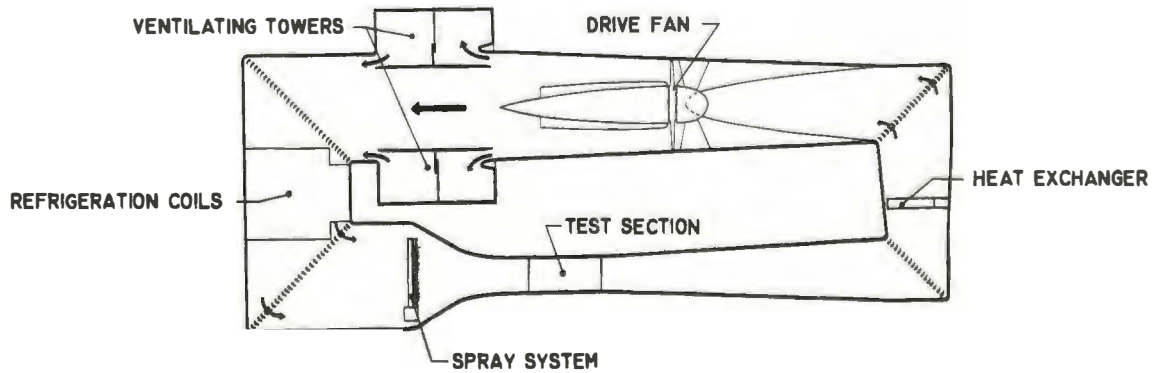
SPRAY SYSTEM

Figure 12.

ICING TUNNEL SPRAY SYSTEM

Figure 13.

MODEL USED TO STUDY AERODYMAMIC PENALTIES
CAUSED BY ICING

Figure 14.

CHANGES IN LIFT AND DRAG CAUSED BY ICING
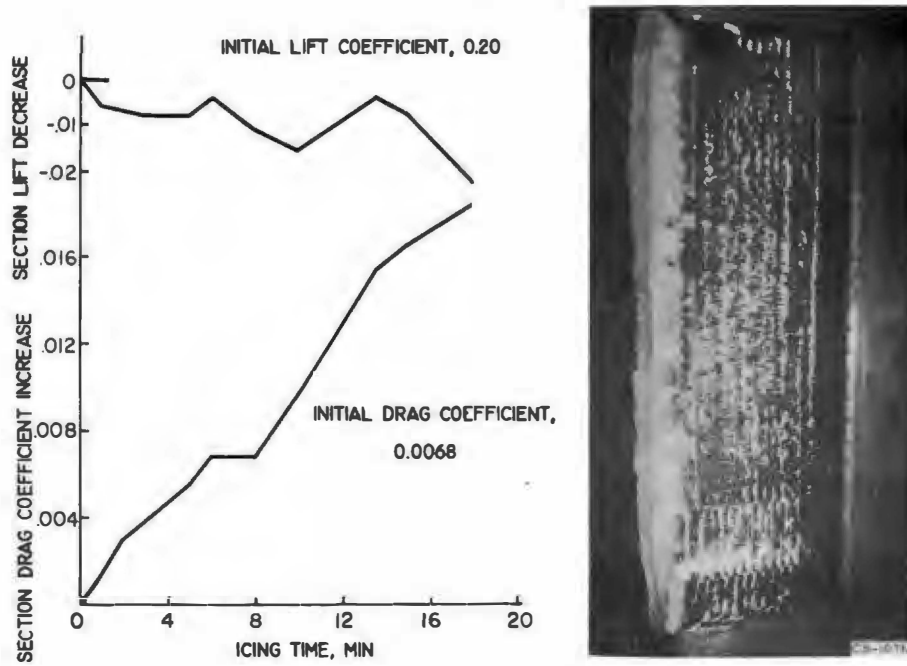
Figure 15.

TYPICAL HEAT LOSSES ASSOCIATED WITH ANTI-ICING
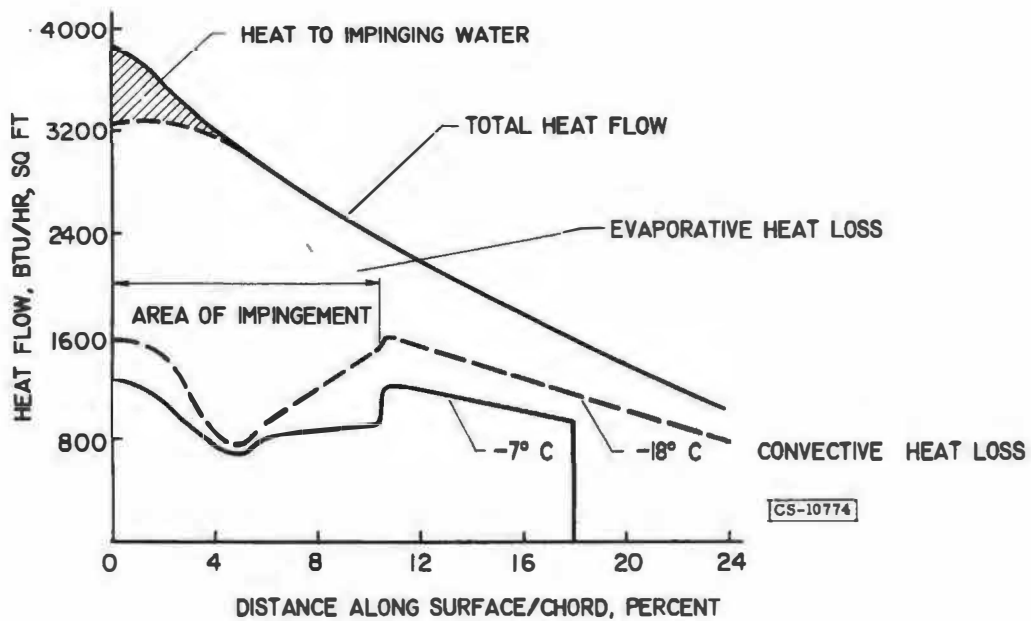
Figure 16.

C-46 AIRCRAFT WITH
THERMALLY ANTI-ICED AIRFOIL MODEL

Figure 17.

TYPICAL ELECTRIC HEATER CONSTRUCTION
FOR C-46 FLIGHT STUDIES
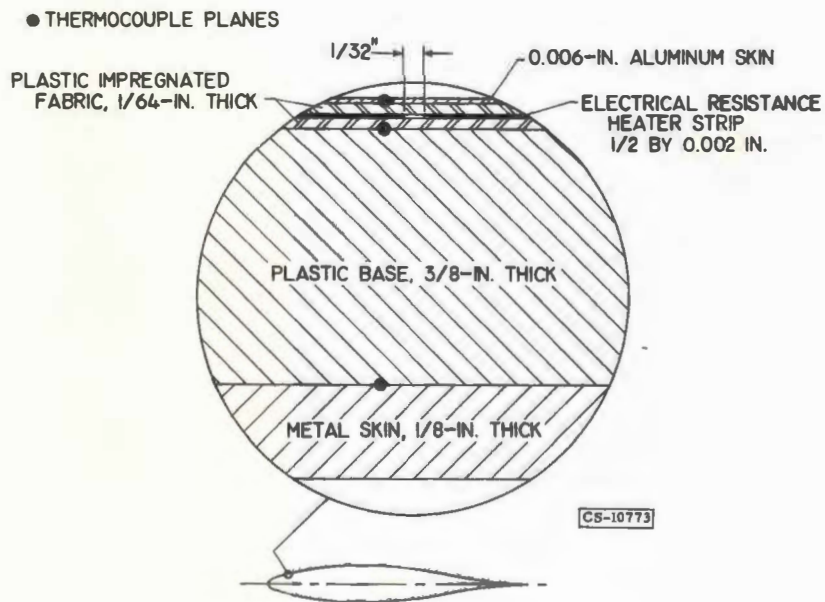
Figure 18.
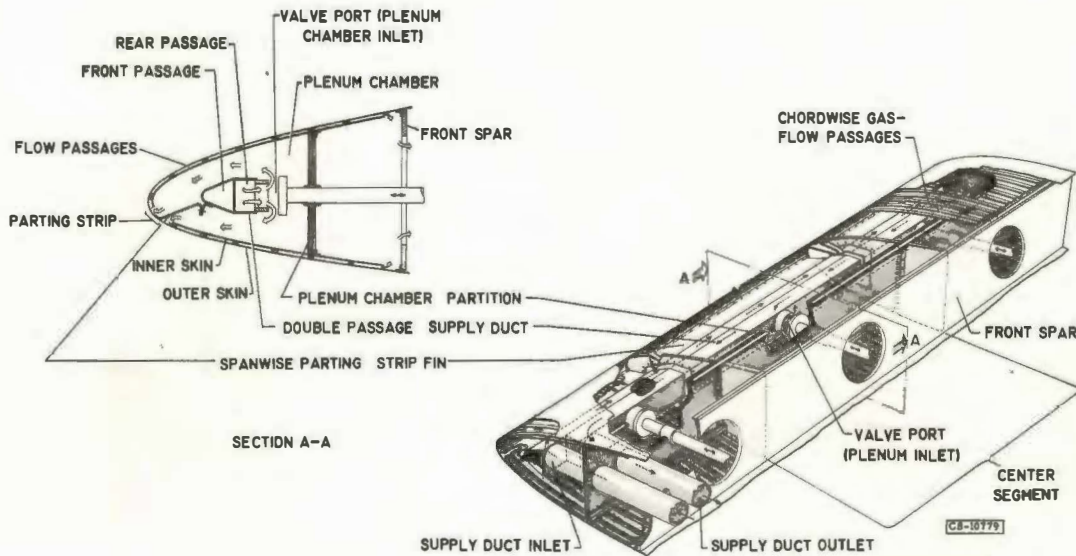
Figure 19.

ICE FORMATIONS ON AIRFOIL BEFORE AND AFTER CYCLIC HEATING

(A) BEFORE HEAT-ON PERIOD   (B) AFTER 15-SECOND HEAT-ON PERIOD

Figure 20.

PNEUMATIC BOOT DE-ICING SYSTEM

Figure 21

ICING PROTECTION FOR PISTON ENGINE-INDUCTION SYSTEM
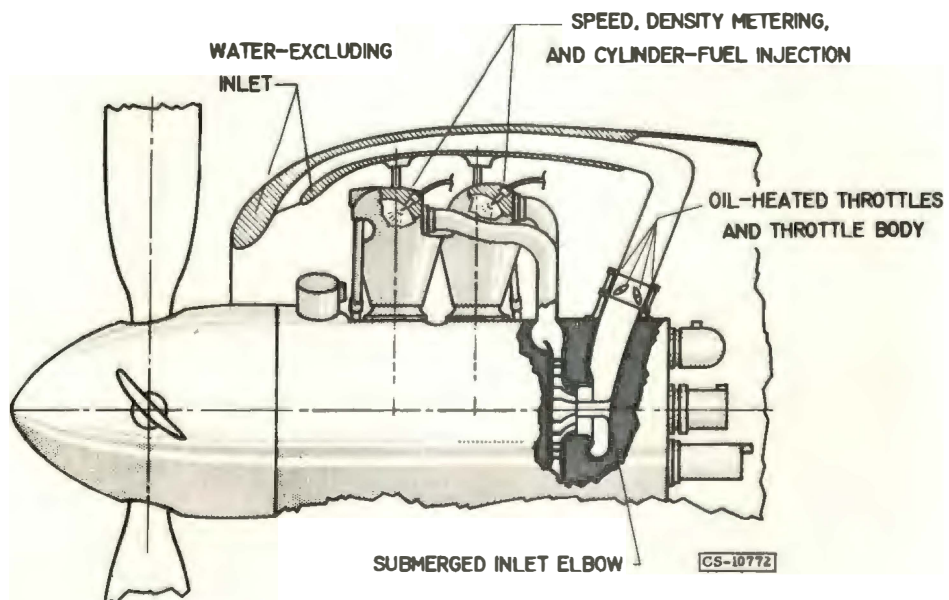
Figure 22.

TYPICAL ICING OF JET ENGINE INLET
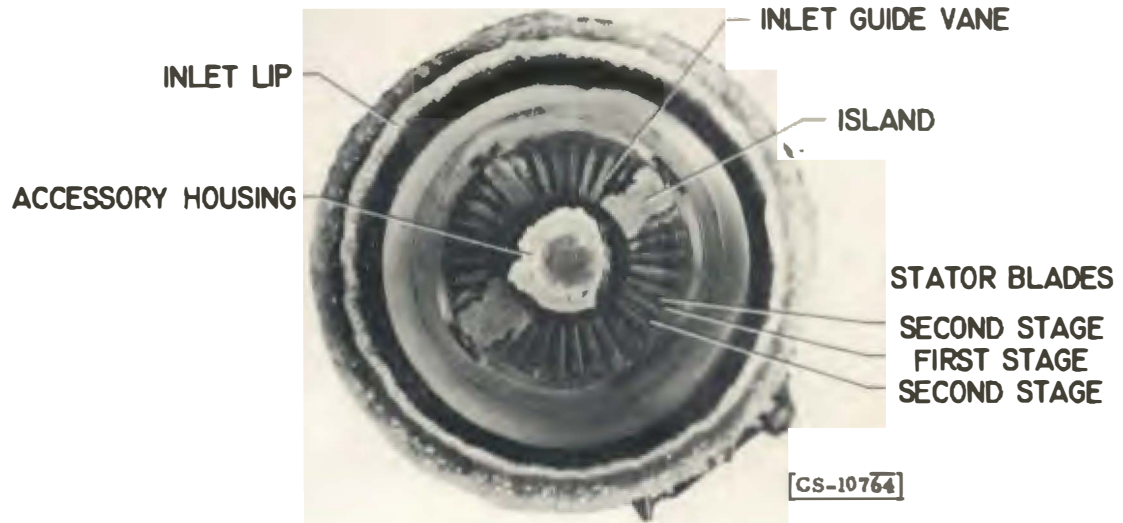
Figure 23.

MODEL USED IN GUIDE VANE STUDIES
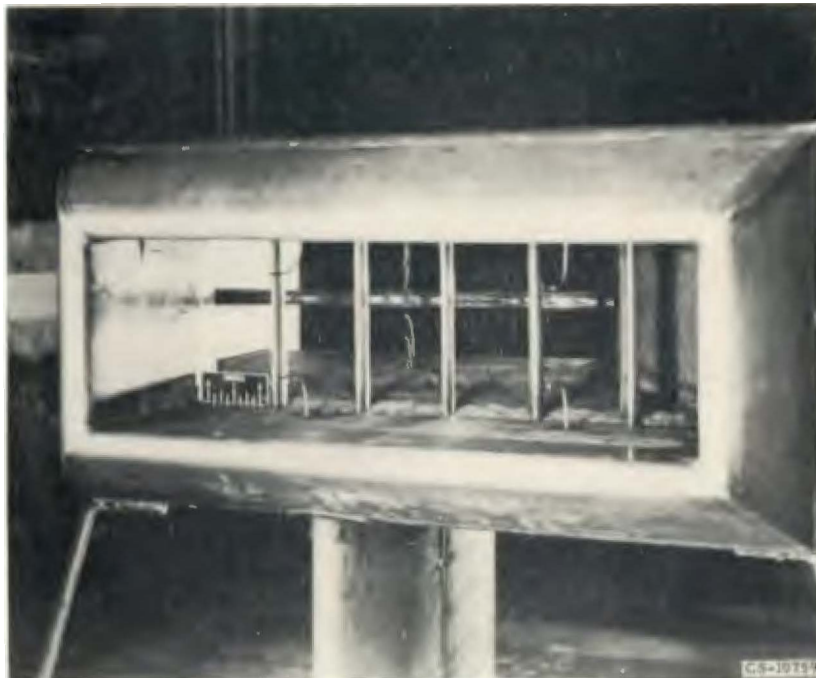
Figure 24.

HEAT SAVINGS OBTAINED BY GUIDE VANE PARTITIONING

TYPICAL HEAT FLOW, BTU/HR
FOR SEVERE ICING CONDITION

(A) VANE I. FULLY HOLLOW

9200

DEAD-AIR SPACE
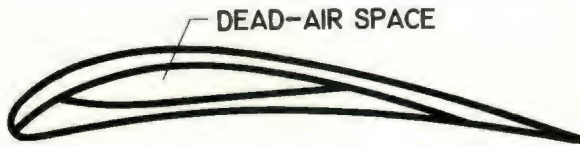
(B) VANE 2. INTERNAL FIN AND INSET

5400

INSERT

(C) VANE 3. INTERNAL INSULATING INSERT

4800

CS-10771

Figure 25.

LEWIS ICING TUNNEL FACILITY

(A) AERIAL VIEW OF ICING TUNNEL.

VENTILATING TOWERS
TEST SECTION
DRIVE FAN
CONTRAVANES
COOLING COILS
TEMPORARY TEST SECTION FOR
PROPELLER ICING RESEARCH
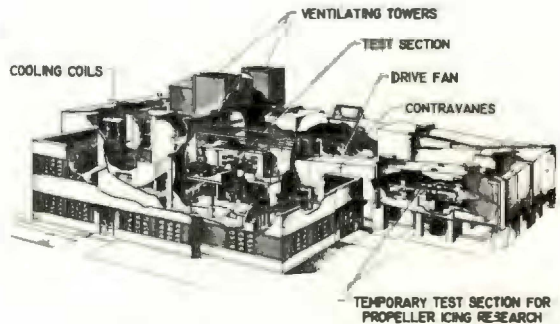
(B) PHANTOM DRAWING OF LEWIS ICING TUNNEL AND OFFICE BUILDING

Figure 26.

CROSS SECTION OF NACA AIR-WATER ATOMIZING SPRAY NOZZLE

STEAM

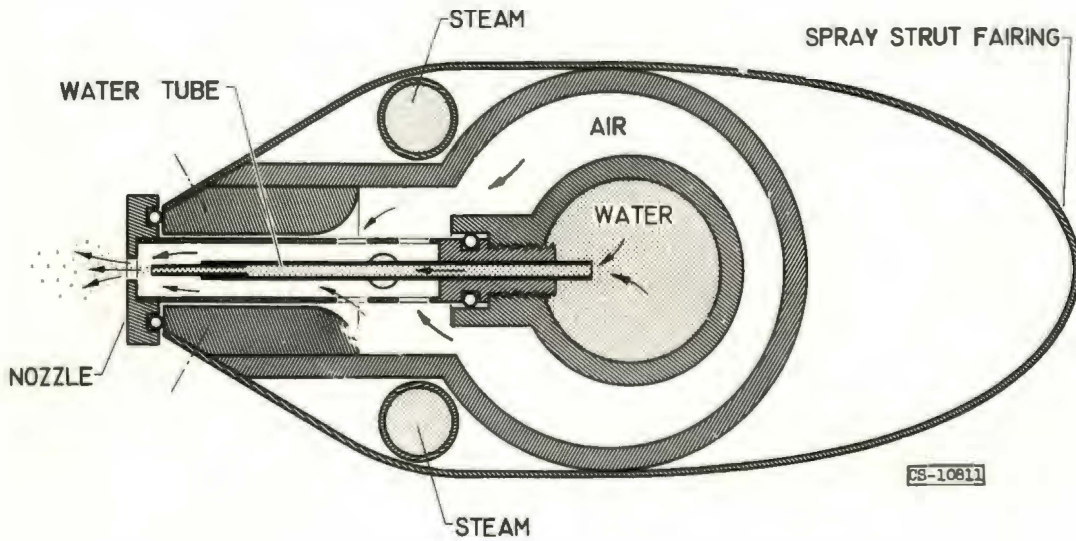SPRAY STRUT FAIRING

WATER TUBE

AIR

WATER

NOZZLE

STEAM

CS-10811

Figure 27.

NACA 3.84x10-INCH HIGH-SPEED ICING DUCT TUNNEL

REFRIGERATED AIR SUPPLY

PLENUM CHAMBER

THERMOCOUPLE PLANE

INLET VALVE

AREA-RESTRICTING METAL BLOCKS

FLOW-STRAIGHTENING TUBES (1" DIA.)

MODEL

6°

10"

48"

12"

TO EXHAUST SYSTEM

96"
TEST SECTION

72"

SCREENS

120"

CS-10805

BELLMOUTH ENTRY

12"
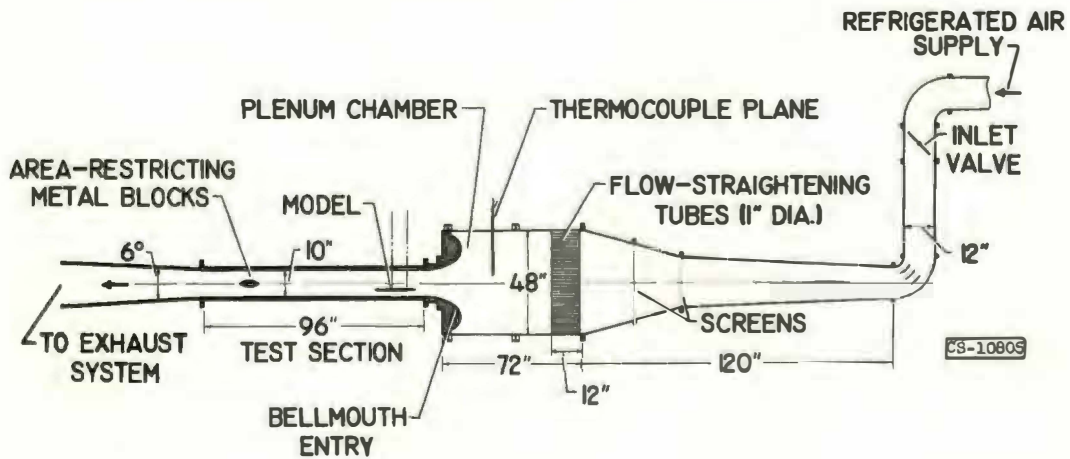
Figure 28.

NACA 12 x 12-INCH HIGH-SPEED ICING DUCT TUNNEL

ALTITUDE EXHAUST

SPRAY NOZZLES

TEST SECTION

ELBOW

SCREENS

REFRIGERATED AIR

STRAIGHTENING VANES

STEAM HEATED THROAT

VARIABLE SECOND THROAT

CS-10812
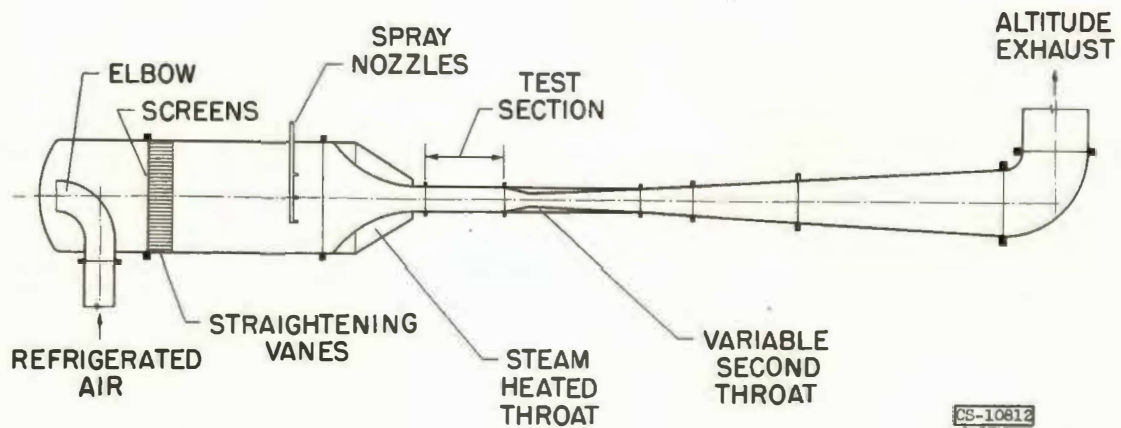
Figure 29.

THERMOCOUPLE INSTALLATION DETAILS

HARDEN POINT

1/8

.015 TO .020 DIA.

PEENING TOOL

1/8 DIA.

NO. 32 AWG GLASS ENAMEL PUSHBACK WIRE

OUTER COVERING

GLASS WRAP

ENAMEL

CURED SILICONE PASTE

SKIN

PEEN HERE AT 6 POINTS AROUND PERIPHERY

.025 TO .050 DIA. TO FIT T.C. BALL

(A) SURFACE THERMOCOUPLE

AFTER SILVER SOLDERING

AFTER HONING

JUNCTION DETAILS

GAS FLOW →

0.06 O.D. × 0.006 WALL STAINLESS STEEL TUBING

NO. 32 AWG COPPER-CONSTANTAN

CS-10817

1/8 LONG 2 HOLE CERAMIC TUBING

(B) AIR FLOW THERMOCOUPLE

Figure 30.

INERTIA-SEPARATION TEMPERATURE PROBE

4 HOLES, 5/32 DRILL

MICARTA INSERT

MOUNTING TUBE

THERMOCOUPLE LEADS

CS-10809

NOSE CAP

IO HOLES, 5/32 DRILL

THERMOCOUPLE JUNCTION
ENCASED IN
STAINLESS-STEEL TUBE

0   1
SCALE, IN.

3817
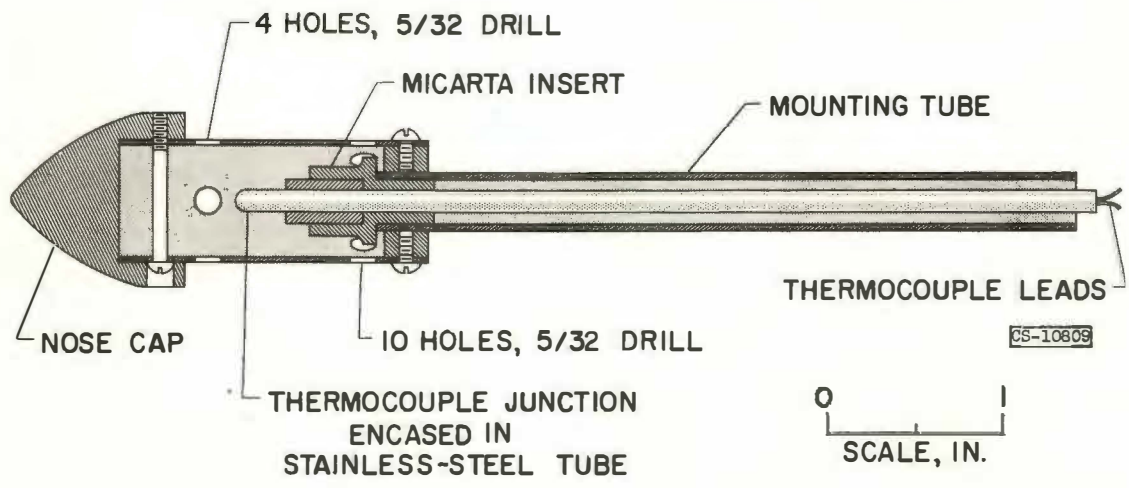
Figure 31

SCHEMATIC DIAGRAM FOR TEMPERATURE MEASURING SYSTEM ON ROTATING BODIES

DISCONNECT PLUGS
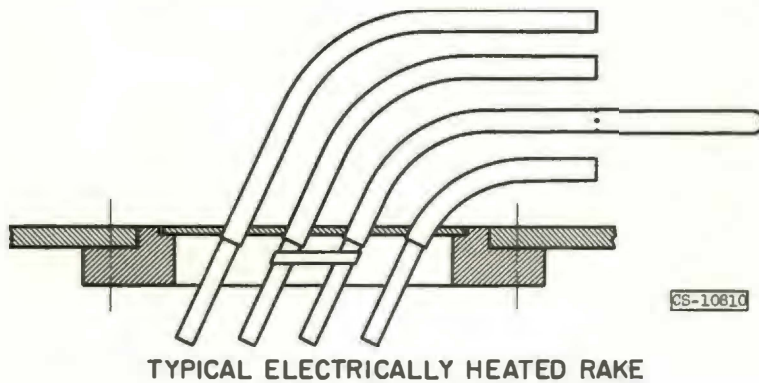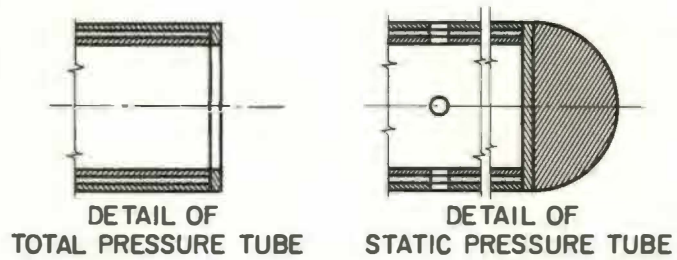
SLIP-RING ASSEMBLY

BRUSH

THERMOCOUPLE

SWITCHING UNIT

Cu   Cu

Cu   Cu   Cu   Cu

TO THERMOCOUPLE
SELECTOR BOX AND
FLIGHT RECORDER

C   C   C   C

Cu   Cu

CS-10814

SPINNER

ROTATING STEAM JACKET

STATIONARY STEAM JACKET
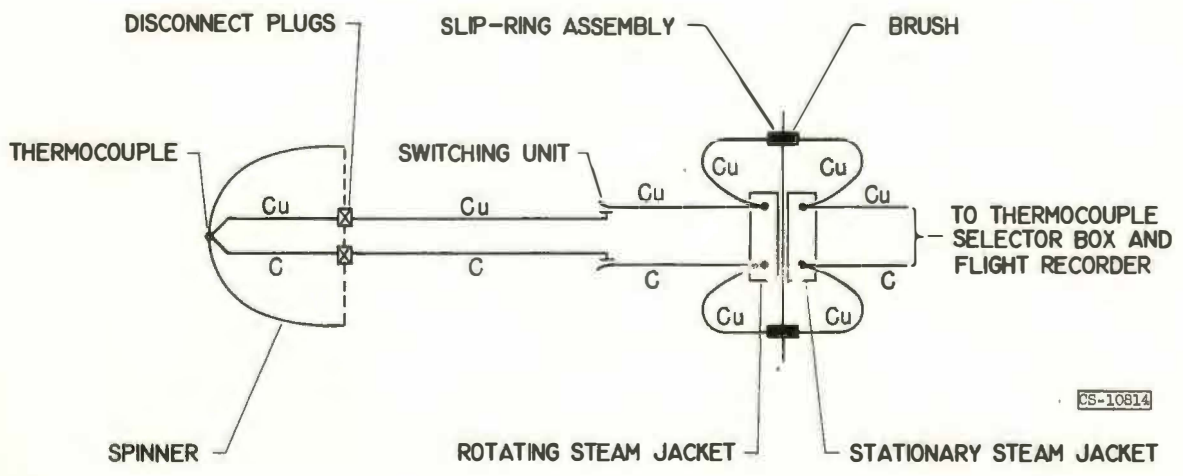
Figure 32

DETAILS OF ELECTRICALLY HEATED PRESSURE TUBES

DETAIL OF
TOTAL PRESSURE TUBE

DETAIL OF
STATIC PRESSURE TUBE

CS-10810

TYPICAL ELECTRICALLY HEATED RAKE

Figure 33

SCHEMATIC DIAGRAM FOR PRESSURE MEASURING SYSTEM
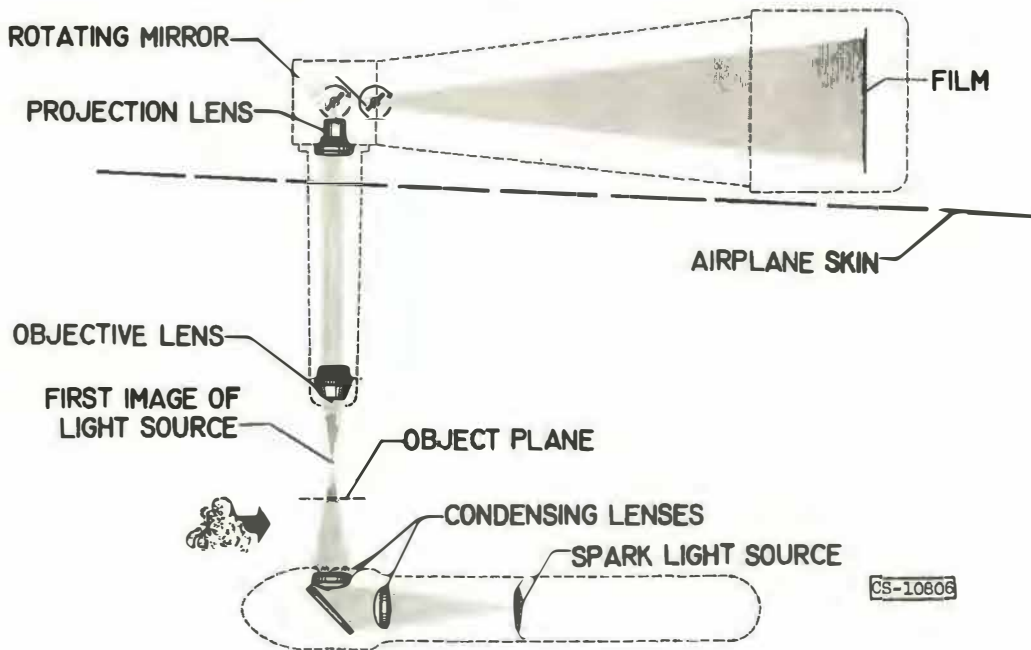## ON ROTATING BODIES

FELT SEAL AND BEARINGS   HOLLOW STATIONARY HOUSING

ROTATING LEADS TO
MODEL PRESSURE TAPS

PRESSURE LEADS
TO MANOMETER

HOLLOW ROTATING SHAFT

CS-10813

→ → DIRECTION OF TRANSMISSION
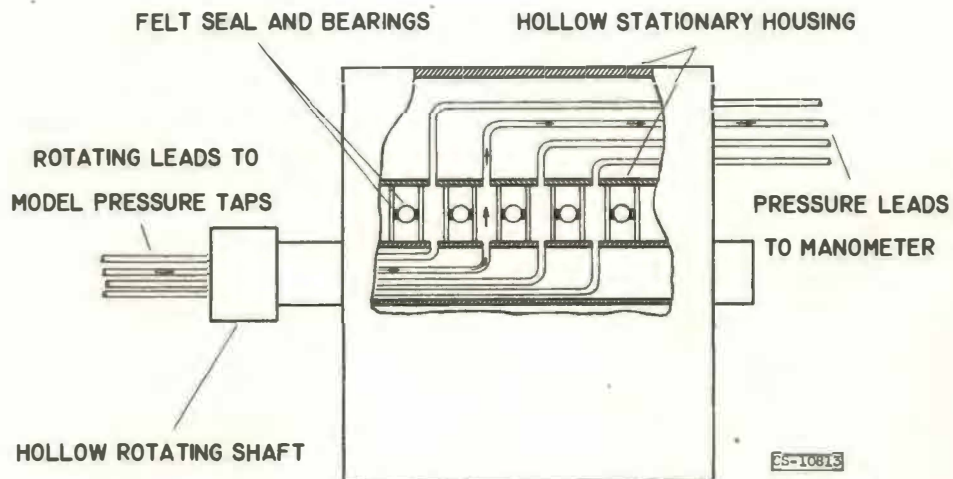
Figure 34

NACA CLOUD CAMERA

Figure 35

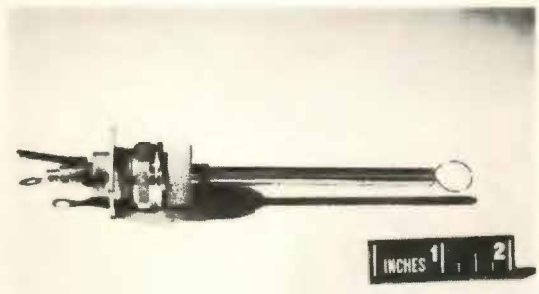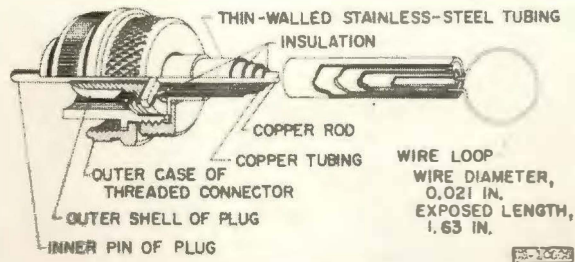# SCHEMATIC SKETCH OF OIL-STREAM AEROSCOPE
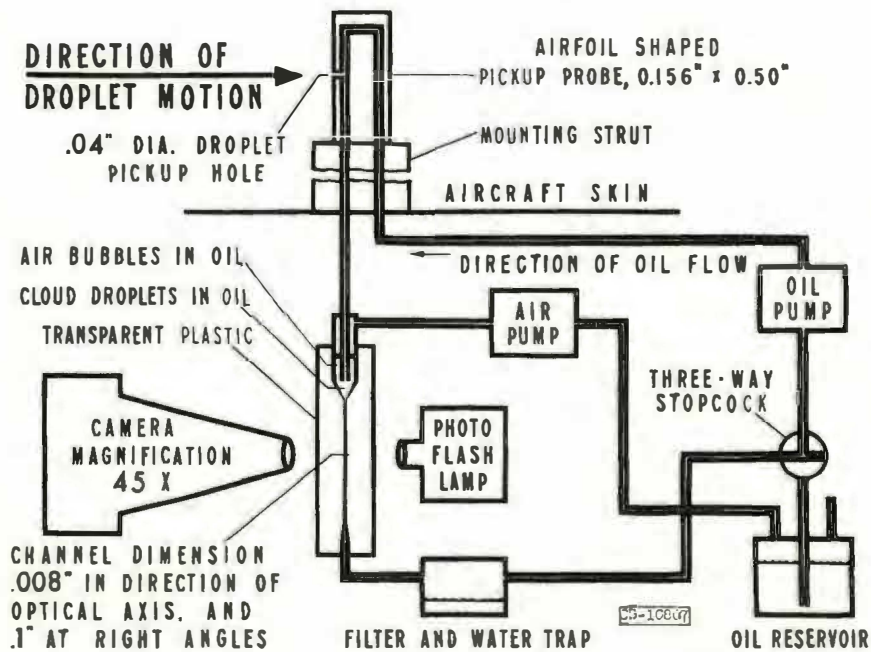
Figure 36

HOT WIRE LIQUID WATER CONTENT METER

(A) WIRE-LOOP AND SUPPORTING-STRUT ASSEMBLY

(B) CONSTRUCTION DETAILS OF WIRE-LOOP ASSEMBLY
AND SUPPORTING-STRUT ASSEMBLY

Figure 37